applied sciences

MDPI

Article

Electrothermal Characteristics of the Electric–Vacuum Heat Pipe in a Low-Pressure Steam Electric Heater: Numerical Modeling and Experimental Study

Rustam Buzyakov, Ali Mekhtiyev, Yelena Neshina *, Valeriy Kalytka * and Oxana Aldoshina *

Energy Systems Department, Abylkas Saginov Karaganda Technical University, Karaganda 100000, Kazakhstan; r.buzyakov@gmail.com (R.B.); barton.kz@mail.ru (A.M.)

* Correspondence: neshinaeg@gmail.com (Y.N.); valerii.kalytka@gmail.com (V.K.); o.aldoshina@ktu.edu.kz (O.A.)

Abstract

This paper examines the electric–vacuum heat pipe (EVHP) as the main heat-transfer component of a low-pressure steam electric heater (LPSEH). The EVHP is interpreted as a wickless, closed, gravity-driven two-phase thermosiphon, in which active electrical power is supplied to the lower evaporation zone, while heat transfer to the outer surface is achieved through the evaporation of the working fluid, steam circulation, condensation and the gravitational return of the liquid phase. The aim of the study is to develop a theoretical and experimental description of the electrothermal regime of the EVHP and to establish the constraints governing the transition from a single smooth tube to a sectional instrument module. The proposed system distinguishes between the electrical input power, the heat generated in the evaporation zone, and the useful heat transferred from the external surface. An external convective–radiative balance was performed, along with numerical modeling in COMSOL Multiphysics and an experimental study on laboratory sections of the LPSEH. It was shown that a single smooth tube with a diameter of 32 mm and a length of 340 mm, at a surface temperature of 90 °C, provides a calculated heat-transfer rate of 16.3–52.8 W for the considered range of convection coefficients and emissivity (24.1–31.8 W under the baseline scenarios at h = 6 W/(m^2·K)). In contrast, removal of 80 W of heat requires an equivalent heat-transfer area of 0.052–0.168 m^2 (0.086–0.114 m^2 under the baseline scenarios). Based on data from the main experimental program MP01–MP40, a regression model of the local temperature regime has been derived, relating the overheating in the upper zone of the section to the specific electrothermal load, the volume of the working fluid and the specific structural mass parameter. For the extended model, R^2fit = 0.911, R^2adj = 0.903, R^2LOO = 0.887, MAELOO = 7.23 °C, and RMSELOO = 8.69 °C were obtained. Additional comparison showed the temperature sensitivity of the mode to the initial residual pressure and to the method of electrical heat supply. The obtained results justify the need for a developed surface, ribbing and sectional regulation of LPSEH. External heat transfer is estimated parametrically in the range of convection coefficient h and emissivity ε, which forms the design range of thermal power and the required surface area. The numerical model is verified by grid independence and energy balance, while the experimental program confirms the main electrothermal trends of the EVHP.

Keywords: low-pressure steam electric heater; electric–vacuum heat pipe; closed gravitational thermosyphon; two-phase heat transfer; active electric power; regression model; local electric heating supply

Check for updates

Academic Editors: Francesco Gabriele Galizia, Marco Bortolini, Mauro Gamberi and Cristian Cafarella

Received: 10 August 2026
Revised: 11 September 2026
Accepted: 15 September 2026
Published: 23 September 2026

Copyright: © 2026 by the authors. Licensee MDPI, Basel, Switzerland. This article is an open access article distributed under the terms and conditions of the Creative Commons Attribution (CC BY) license.

1. Introduction

In recent years, electric heating has increasingly been regarded not merely as an auxiliary heating technology, but as an independent element of energy conversion in buildings, industrial facilities, and local heat supply systems. The reason is that the electric heating device is simultaneously a receiver of electric energy, a load-controlled power supply system and a local heat source. Therefore, its efficiency cannot be evaluated only by the fact of converting electric energy into heat; it is necessary to take into account the controllability of active power, the dynamics of reaching the mode, the uniformity of the temperature field, the safety of the accessible surface, the quality of electric energy consumption and the possibility of working in autonomous or hybrid heat supply schemes.

The study focuses on the electrothermal interaction inside the local heater: controlled active power supply, two-phase heat transfer and the formation of a safe heat-radiating surface. National energy policy, power-to-heat and demand flexibility are considered as an applied context for the use of the developed solution [1–52].

In the context of this problem, it is important to compare not the total efficiency of direct electric heating, but the path of heat transfer from the local heater to the accessible surface. In a conventional resistive element, this path is determined by the thermal conductivity of the case and external convection; an oil radiator equalizes the field due to the heat capacity of the liquid medium, but increases inertia; EVHP uses passive evaporative-condensation transfer without an external water circuit and thereby allows the structural separation of the local area of electrical heat supply and a developed heat-transfer surface [12,33,34,53–66]. It is this advantage, and not exceeding the law of energy conservation, that motivates the use of EVHP in LPSEH.

One of the directions for increasing the functional efficiency of local electrical heating devices is the use of an internal two-phase heat-transfer element. Heat tubes and closed two-phase thermosyphons transfer heat due to evaporation of the working medium in the heat supply zone, movement of steam to the condensation zone, release of latent heat of vaporization and return of the liquid phase [5–10]. Due to this, a significant heat flux can be transferred at a relatively small temperature difference, and the local electric heating zone can be separated from the developed heat-radiating surface.

The development of the theory and practice of heat pipes shows that the effectiveness of such devices is determined not only by the material of the casing, but also by the working medium, the degree of filling, orientation, geometry of the evaporation and condensation zones, external convection conditions, the presence of non-condensable gases, condensate return modes and maximum thermal loads [6–14]. For heating devices, a wickless gravity scheme is especially important, in which the return of the liquid phase is provided by gravity. Such a scheme is structurally simpler than a capillary heat pipe, but requires vertical or close to vertical orientation, stable condensate return and prevention of dry running of the evaporation zone [8–10,13,14].

In construction and heating applications, heat pipes are used to redistribute heat in radiators, low-temperature heating systems, terminal devices and hybrid heat supply schemes [12,33,34]. Their advantage is manifested not in violation of the law of energy conservation, but in a change in the heat-transfer path: locally supplied power is distributed over a larger surface, the temperature gradient decreases, the output of individual zones to the mode accelerates, and the possibility of constructive separation of the heating unit and the available surface of the device increases [5,12,33,34].

Low-pressure steam electric heater (LPSEH) belongs to this class of devices. Its main heat-transfer element is an electric–vacuum heat pipe (EVHP)—a sealed vertical evacuated pipe with a limited amount of distilled water, a lower zone of electric heat supply, an evaporation zone, a vapor channel, a condensation zone and a gravitational condensate

return. Previous works and patent solutions on electric–vacuum heating elements and radiators with EVHP confirmed the feasibility of the scheme [15–18,28–32]; this study develops its design basis, experimental identification and sectional design principles.

The term "low-pressure" in this work is associated with the initial evacuation of the internal cavity and with the working evaporation–condensation cycle of water vapor at temperatures characteristic of heating devices. The working pressure in the sealed cavity is determined by the saturation temperature of the working medium; therefore, a correct description of the EVHP requires the use of thermodynamic properties of water and water vapor, taking into account phase equilibrium and joint consideration of internal heat transfer and external heat transfer [19]. For numerical analysis of such a problem, it is advisable to use a multiphysics simulation, including the thermal conductivity of solid elements, steam–liquid transfer, convection, radiation and boundary conditions for heat exchange with the room [20–22].

In this article, the expression "low-pressure" characterizes the technological initial evacuation and the design temperature range of the surface of 70–90 °C. In forced laboratory modes, the pressure of the steam component is determined by the water saturation temperature, which allows the use of an extended temperature range for the study of heat transfer and the design boundaries of the EVHP.

The development history, design solutions and previously published experimental data of the EVHP/LPSEH family are presented in [15,16,18,28–32]. Theoretical provisions on two-phase heat transfer, thermosyphons, external heat exchange and numerical modeling are additionally based on independent sources [5–14,19–24,33,34,67], forming a balanced methodological basis for the study.

Critical Literature Analysis and Research Gap

Classical models of heat pipes and thermosyphons describe in detail phase equilibrium, thermal resistance, hydrodynamic limits and the influence of orientation and filling [5–14]. The present work develops this theoretical basis for an EVHP with a built-in electric heat input, introducing active electric power as an independent input parameter. For heat tube heating terminals, the advantages of a developed surface and rapid redistribution of heat were previously shown [12,33,34]; in this formulation, these provisions are combined into the connection "active power–evaporation zone–temperature field EVHP–external convective–radiation balance." Previous publications on EVHP/LPSEH [15–18,28–32] are supplemented by calculation of heat-transfer area, uncertainty assessment and a statistical model of temperature regime.

The key scientific and technical task consists of a coordinated description of the active electric power of the heating unit, localization of heat supply in the evaporation zone, temperature distribution over the casing, available heat-emitting surface, the amount of working medium, the initial residual pressure and the geometry of the section [5–18,28–34]. This combination of parameters forms the calculated basis for the transition from a single laboratory EVHP to a sectional device of a given power.

The experimental program combines thermal and measuring aspects: temperature series, active power, voltage, current, section mass, geometry, fill volume and initial residual pressure are recorded in a single test system, and statistical processing takes into account inter-sample variation and measurement uncertainty [26,27]. The local temperature of the bare laboratory EVHP is used to identify the electrothermal model, and the temperature of the accessible surface of the instrument module is used to design finning, casing and temperature safety [23–25].

Thus, the scientific and technical task of the study is to form a consistent computational and experimental description of EVHP/LPSEH as an electrothermal unit in which active

electric power is converted to heat in the evaporation zone, transferred by an internal two-phase mechanism and removed by an external convective–radiation surface. Within the framework of this statement, the limit specific load, the required heat-transfer area, the effect of initial evacuation and working fluid parameters, as well as the engineering interpretation of the experimental regression model are determined.

The purpose of this article is to develop a physical, mathematical and numerical description of the electrothermal mode of the electric–vacuum heat pipe of a low-pressure steam electric heater, including active electric heat transfer, internal two-phase transfer, external heat exchange and calculation of the required heat-transfer area, and to compare the design consequences of the model with experimental data. The contribution of the article is as follows: the energy production of EVHP as an electrothermal unit has been formed; calculation of the external heat-transfer limit of a smooth single tube was performed; numerical modeling of single-phase and two-phase modes was carried out; experimental data for LPSEH sections were summarized; a regression model of the temperature regime was built; the transition to a developed surface and sectional construction of a device for a target power of 80 W per section is justified.

This article discusses the thermophysical and electrothermal basis of the EVHP as an independent LPSEH heat-transfer unit. The obtained patterns are directly used in the design of the sectional instrument module, the choice of a developed heat-emitting surface, control parameters and temperature modes.

2. Materials and Methods

2.1. EVHP Physical Diagram as Heat-Transfer Unit of LPSEH

In this work, EVHP is formalized as a vertical closed wickless gravitational two-phase thermosyphon. The design setting is axisymmetric; working medium—water; casing—copper; the electric heater is represented by an equivalent heat flow in the evaporative section, 40 mm long. For the phase-to-phase boundary, the local equilibrium $p_v = p_{sat}(T_i)$ is assumed. The return of condensate along the wall in an axisymmetric numerical model is described by an equivalent Brinkman layer that reproduces the hydrodynamic function of a liquid film. The effect of non-condensable gases is considered experimentally through the initial residual pressure.

The conservation of mass in the liquid and vapor regions is given by the equation [8–10,20,21]:

$$\partial\varrho/\partial t + \nabla\cdot(\varrho v) = 0. \quad (1)$$

The momentum balance is written in standard Newtonian form [8–10,20,21]:

$$\varrho(\partial v/\partial t + v\cdot\nabla v) = -\nabla p + \nabla\cdot[\mu(\nabla v + \nabla v^T)] + \varrho g. \quad (2)$$

The energy balance of the moving medium is used in enthalpy form [8–10,20,21]:

$$\varrho\partial h/\partial t + \varrho v\cdot\nabla h = \nabla\cdot(\lambda\nabla T) + q_v + Dp/Dt. \quad (3)$$

For a solid casing at $v = 0$, the equation of thermal conductivity $\varrho c_p\partial T/\partial t = \nabla\cdot(\lambda\nabla T) + q_v$ is applied, and for liquid and vapor phases—$\varrho c_p(\partial T/\partial t + v\cdot\nabla T) = \nabla\cdot(\lambda\nabla T) + S$. Interfacial transfer is closed by the balances $\dot{m}_v = Qlat/hfg$, $m''ev + m''cond = 0$ and $q''lat = m''hfg$. The Hagen–Poiseuille equation is used to estimate vapor motion, and the equivalent return of the liquid phase is described by the Brinkman equation: $-\nabla p_l + \mu_l\nabla^2 u_l - (\mu_l/K)u_l + \varrho_l g = 0$ [8–10,20–22].

The scope of installation covers a closed vertical EVHP with a water working fluid and gravitational return of condensate. The model is used to analyze the electrothermal

balance, temperature distribution and design limit of external heat transfer. Casing strength, non-condensable gas dynamics and critical hydrodynamic conditions are considered as independent design blocks in the subsequent structural design.

The investigated EVHP (Figure 1) is a sealed vertical element partially filled with distilled water. Before sealing, air is removed from the inner cavity; the initial residual pressure sets the content of non-condensable gases and affects the start of the evaporation–condensation cycle. An electric heating element is arranged in the lower zone to localize heat feed to the nearby liquid phase.

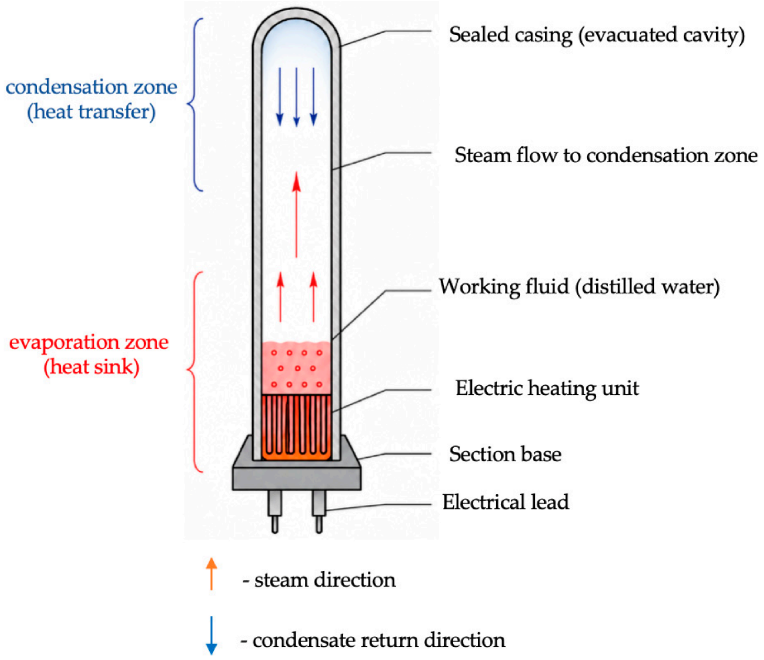


Figure 1. Schematic diagram of EVHP section based on gravity-based LPSEH.

In the operating mode, the liquid phase in the evaporation zone is heated to saturation. The generated steam moves upward into the condensation zone, where it gives off latent heat of vaporization to the inner wall of the casing. The condensate returns downward by gravity. Such a scheme does not require a wick and a circulation pump, but is sensitive to orientation, degree of filling, content of non-condensable gases and external conditions of heat transfer.

The term "low pressure" refers to the technological initial vacuum and design mode of the outer surface of 70–90 °C, for which the pressure of saturated water vapor is approximately 0.031–0.070 MPa [19]. Forced laboratory modes of the bare section cover a higher temperature range and are used to analyze the stability of heat transfer and determine the design parameters of the finished device.

In the program MP01–MP40, the initial residual pressure before heating was recorded, and the operating pressure of the heated cavity was estimated by the water saturation temperature under the condition of local phase equilibrium. This approach allows a consistent interpretation of temperature conditions and the steam component of the internal pressure in the studied range.

The local phase equilibrium at the liquid–steam interface is given by (4):

$$p_v = p_{\text{sat}}(T_i) \tag{4}$$

where p_v—steam phase pressure at the interfacial surface, Pa; p_{sat}—saturated steam pressure of the working fluid, Pa; T_i—interfacial surface temperature, K.

2.2. Electrical Power Model for Active Power Supply

For a correct description of the LPSEH, it is important to separate three quantities: the active electrical power consumed by the heating unit from the network; thermal power actually localized in the evaporation zone; useful heat transfer of the selected external surface. Their equality is possible only in the idealized stationary case with the absence of losses and the complete coincidence of the selected surface with the full heat-emitting surface of the device.

In the resistive case, where the voltage and current are sinusoidal, the active power is determined by the conventional expression [35,59]:

$$P_{\text{el}} = U_{\text{rms}} I_{\text{rms}} \cos\varphi \tag{5}$$

where U_{rms}—actual voltage value, V; I_{rms}—effective current, A; $\cos\varphi$—power factor.

For non-sinusoidal modes, phase-pulse control or power converter, active power is set as the average value of instantaneous power [35–37]:

$$P_{\text{el}} = \frac{1}{T}\int_0^T u(t) i(t)\, dt \tag{6}$$

The power supplied directly to the evaporation zone can be expressed in terms of the localization factor η_{ev} [23,24]:

$$Q_{\text{ev}} = \eta_{\text{ev}} P_{\text{el}}, \quad 0 \le \eta_{\text{ev}} \le 1 \tag{7}$$

The effective heat transfer of the selected external surface is determined by the coefficient η_{use} [23,24]:

$$Q_{\text{use}} = \eta_{\text{use}} P_{\text{el}} \tag{8}$$

The η_{use} factor characterizes the fraction of active power related to the selected design external surface. For a fully placed electric heater, the total consumed power is converted into room heat, and the introduction of η_{use} allows the external limit of a specific heat-emitting surface to be calculated separately and its area to be selected correctly.

2.3. External Energy Balance and Required Heat-Transfer Area

The external surface of the EVHP gives heat to the air and surrounding surfaces of the room due to free convection and thermal radiation. For engineering evaluation, the external heat flux density is given by the sum of convective and radiation components [23,24]:

$$\begin{gathered} q_s = h(T_s - T_a) + q_{\text{rad}} \\ q_{\text{rad}} = \varepsilon\sigma(T_s + 273,15)^4 - \varepsilon\sigma(T_r + 273,15)^4 \end{gathered} \tag{9}$$

where q_s—heat flow density, W/m^2; h—convective heat-transfer coefficient, W/(m^2·K); T_s—surface temperature, °C; T_r—radiation temperature of surrounding surfaces, °C; ε—degree of surface blackness; σ—Stefan-Boltzmann constant; q_{rad}—radiation component of heat flow density, W/m^2.

$$Q_{\text{out}} = \int_A q_s\, dA \tag{10}$$

$$A_{\text{req}} = \frac{Q_{\text{target}}}{q_s} \tag{11}$$

The lateral surface area of a smooth cylindrical tube is given by the expression [23,24]:

$$A_0 = \pi DL \quad (12)$$

where D—outer diameter, m; L—length of the heat-transfer section, m. For a tube with a diameter of 32 mm and a length of 340 mm, A_0 is approximately 0.034 m^2. It is this value that is used as a reference when assessing the capacity to dissipate 80 W without finning.

The free convection coefficient h and the emissivity ε are specified as engineering boundary conditions for the parametric analysis: h = 4–18 W/(m^2·K), ε = 0.10–0.90; the baseline scenarios use h = 6 W/(m^2·K), whilst the COMSOL verification mode uses h = 8 W/(m^2·K), ε = 0.50. The resulting values of Q_{out} and A_{req} define the calculated design range for external heat transfer and enable an assessment of the sensitivity of the energy balance to the surface condition and natural convection conditions.

Parameters of the studied EVHP are preseted in Figure 2 ans summarized in Table 1.

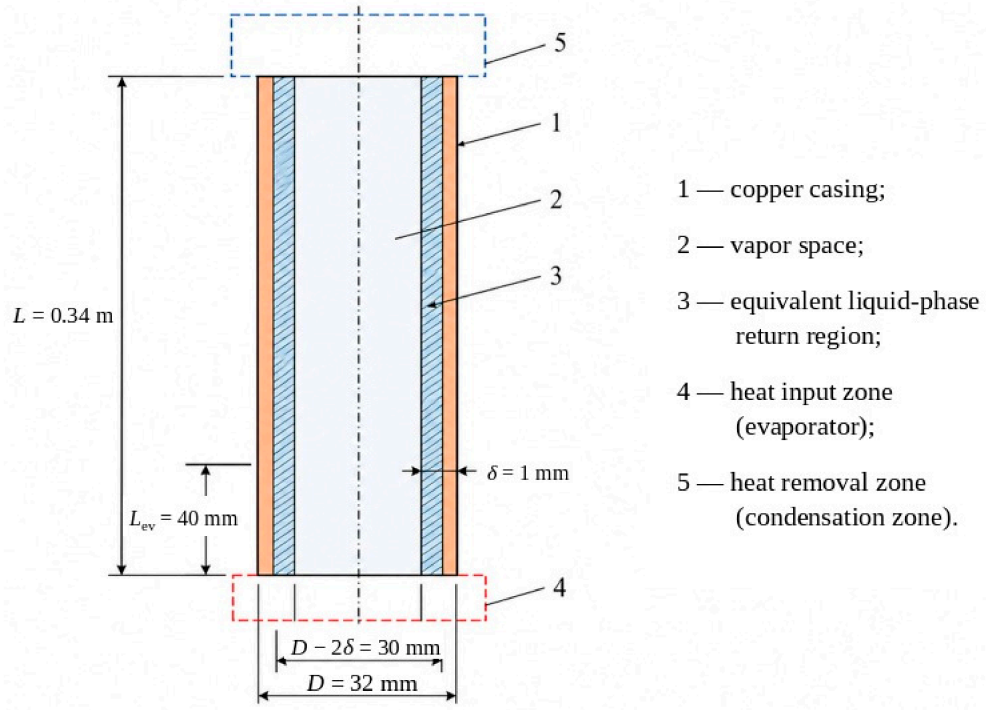


Figure 2. LPSEH EVHP axisymmetric design area.

Table 1. Geometric and design parameters of a single EVHP.

Parameter	Designation	Value	Comments
Calculation area length	L	0.34 m	Single lab tube geometry
Outer diameter	D	32 mm	Control version of smooth EVHP
Wall thickness	δ	1 mm	Constructive assumption
Evaporation zone length	L_{evop}	40 mm	Local heat supply area
Casing material	-	copper	High thermal conductivity of the wall
Working fluid	-	distilled water	Low and medium temperature range
Air temperature	T_a	20 °C	Space boundary condition
Convection coefficient	h	6; 8; 18 W/(m^2·K)	Free and improved heat-transfer scenarios
Degree of blackness	ε	0.10; 0.50; 0.90	Bare, treated and painted surface

2.4. Numerical Model in COMSOL Multiphysics

Numerical modeling was used to verify the qualitative difference between single-phase and two-phase modes. The design area includes a copper wall, internal steam

cavity, liquid area and evaporation zone. The thermophysical properties of water and water steam are set according to IAPWS-IF97 [19], and the numerical implementation is based on the modules of heat transfer, hydrodynamics and porous media in COMSOL Multiphysics [20–22]. The software package version is COMSOL Multiphysics 6.4.

The electric heat supply in the design setting is represented by equivalent heat flow in the evaporation zone, which provides a direct simulation of the subsequent heat transfer from the active power input zone to the outer surface. For the induction version, the relationship between the input power and the core power is additionally taken into account in the analysis of dynamic experiments.

The model uses two control modes. The first mode is single-phase, without evaporation and condensation; it shows the temperature gradient that would occur in the absence of a phase transfer mechanism. The second mode is two-phase, with equivalent transfer of latent heat and condensate return; it demonstrates the smoothing of the temperature field along the height of the tube. The energy gap is controlled by an independent balance of heat input, external heat dissipation and internal energy change [8–10,20–22].

$$P_{ev} - Q_{out} - \frac{dU}{dt} = \Delta Q_{bal} \quad (13)$$

In the stationary calculation, $\frac{dU}{dt} = 0$; therefore, the consistency of the supplied power and external heat transfer is checked. A non-stationary single-phase calculation is used to demonstrate temperature localization when phase transfer is disabled.

Calculations are made in COMSOL Multiphysics 6.4. Design geometry: length 340 mm, outer diameter 32 mm, copper wall thickness 1 mm, evaporation zone length 40 mm; ambient temperature 20 °C. An integral heat supply of 80 W was set in the evaporation section. Free convection and radiation were used on the outer surface; in the two-phase test case, h = 8 W/(m^2·K) and ε = 0.50 were used. Thermophysical properties of water and steam were set according to IAPWS-IF97 [19]. Two-phase control mode was calculated in stationary, single-phase comparative mode and in non-stationary mode.

Grid independence was verified by successive grinding of the design grid. During the transition from the basic to the refined grid, the maximum temperature changed from 185.2 to 184.8 °C (by 0.4 °C), the estimated external heat transfer—from 80.5 to 80.1 W, and the integral energy error decreased from 0.6 to 0.1%. For the coarse mesh, the corresponding values were 188.3 °C, 82.4 W and 3.0%. Additionally, varying the K equivalent permeability from 10^{-12} to 10^{-10} m^2 gave T_{max} = 186.5–184.5 °C and Q_{out} = 80.0–80.1 W without the appearance of dry zones in the numerical solution (Table 2). Methodologically, the description of the grid, boundary conditions and numerical verification is given in the form recommended for reproducible CFD studies (Table 3) [67].

Table 2. Verification of the stability of the numerical result as the mesh size is reduced (Q_{in} = 80 W).

Grid Level	T_{max}, °C	$T_{s,avg}$, °C	Q_{out}, W	Change in T_{max}, °C	Energy Imbalance, %
Coarse	188.3	187.5	82.4	—	3.0
Basic	185.2	184.6	80.5	3.1	0.6
Refined	184.8	184.3	80.1	0.4	0.1

The numerical solution was evaluated by two integral reproducibility criteria: grid stability and energy balance. For basic and refined grids, the energy error is less than 1%, and the change in the maximum temperature during grid grinding is 0.4 °C, which confirms the stability of the calculated result.

Table 3. Metrological characteristics and accepted uncertainty of key quantities.

Value	Product/Base	Accepted Uncertainty	Comments
Temperature/ΔT	Contact thermocouples; ST RK 2.87-2005	UΔT ≈ 4.2 °C	Extended instrumental evaluation of the temperature channel regulatory characteristic
Active power, P	Wattmeter up to 500 W	δP ≈ ±2%; uP ≈ 0.69/0.92/1.15 W for 60/80/100 W	The standard uncertainty is calculated using a uniform distribution
Specific load, q	Calculation based on P and the geometry	about 5–6%	Composite calculated value
Initial pressure, p_0	Vacuum gauge before heating	monitoring of the technological initial state	The initial pressure is recorded by the vacuum meter; the working steam component is estimated by saturation temperature
Voltage and current	Digital multimeters	used as control electrical channels	Control electrical channels are used for comparison of active power modes

For a shapeless gravitational thermosyphon, the operating range is estimated according to the condition $Q_{in} \leq \min\{Q_{return}, Q_{boil}, Q_{entr}, Q_{ext,lim}\}$, which combines stable condensate return, boiling, liquid entrainment and external heat removal. With a power of 80 W and a length of the evaporator of 40 mm, the heat flow along the cylindrical surface with a diameter of 32 mm is approximately 19.9 kW/m^2 (about 20–21 kW/m^2). Numerical verification of K equivalent permeability sensitivity showed stable formation of return flow in the studied modes. Quantitative identification of hydrodynamic limits is included in the program of further expansion of the operating range of the EVHP [8–10,13,14].

In addition to the basic comparison of single-phase and two-phase modes, a parametric analysis of external boundary conditions was performed. With unchanged geometry and Ts = 90 °C, the convection coefficient varied in the range h = 4–18 W/(m^2·K), and the emissivity—ε = 0.10–0.90; Q_{out} = 16.3–52.8 W and A_{req} = 0.052–0.168 m^2. The obtained analysis confirms the stability of the design conclusion to the change in external heat exchange and forms the basis for an extended CFD study of the effect of geometry, degree of filling and power.

2.5. Pilot Plant and Test Program

Experimental studies were carried out on a laboratory bench that provides dosed filling of the working fluid, evacuation of the internal cavity, supply of active electric power and recording of the temperature response. Voltage, current, active power, temperature, initial residual pressure, mass and geometric parameters of the section were monitored.

The main program included 40 batches of MP01–MP40 (main program). Active power of 60, 80 and 100 W, working fluid volume of 10 and 15 mL, outer diameter of 20, 28 and 32 mm, length of 25–45 cm and dry weight of 235–573 g were varied. The initial residual pressure in the main sample was 9.807 kPa. Additional batch AP01-AP19 (additional program) at p_0 = 5.066 was used for separate evaluation of the vacuum depth impact (Table 4).

Table 4. Factor ranges for the main experimental program MP01–MP40.

Parameter	Designation	Range/Levels	Purpose
Active electric power	P_{el}	60; 80; 100 W	Mode electric factor
Working volume	V	10; 15 mL	Process factor of filling
Outer diameter of the section	D	20; 28; 32 mm	Geometric factor
Section length	L	25–45 cm	Defines the surface area
Dry weight of section	m	235–573 g	Structural mass factor
Initial residual pressure	p_0	9.807 kPa	Main selection condition
Bare side surface area	A_0	0.0157–0.0452 m^2	Power normalization
Specific electric heat load	q	1326.3–3819.7 W/m^2	Major energy predictor
Unit weight	μ	10.04–14.96 kg/m^2	Construct-mass predictor
Local temperature of the upper zone	T_{final}	85.0–191.0 °C	Dependent variable

The MP01–MP40 experimental program is structured as a screening matrix of actually manufactured sections and comprises 22 tests at 60 W, 13 at 80 W and 5 at 100 W. The geometry and mass of the samples vary according to the design configurations, ensuring a wide range of specific electrothermal loads. The overall average temperature of 142.6 °C was calculated across all 40 runs, whilst group averages by power are used for further comparison. The complete MP01–MP40 matrix is given in Supplementary Table S1.

Metrological assessment was performed according to archival test protocols and requirements [26,27]. Active power was monitored using a wattmeter with a range up to 500 W and a maximum relative error of approximately ±2%; the standard uncertainty of power, following a uniform distribution, is approximately 0.69 W at 60 W, 0.92 W at 80 W and 1.15 W at 100 W. For the final value of the temperature rise, an expanded instrumental uncertainty of $U\Delta T \approx 4.2$ °C was adopted, whilst the relative uncertainty of the calculated specific load q is of the order of 5–6%. These characteristics are used in assessing the reliability of the temperature dependencies and the regression model.

Uncertainty propagation during processing is carried out in accordance with GUM [27]. For the overheating $\Delta T = T_{final} - T_{room}$, the standard uncertainty is estimated as $u(\Delta T) = [u^2(T_{final}) + u^2(T_{room})]^{1/2}$. Since $q = P/(\pi DL)$, the relative standard uncertainty is determined by the expression $u(q)/q = [(uP/P)^2 + (uD/D)^2 + (uL/L)^2]^{1/2}$; similarly, for $\mu = m/(\pi DL)$: $u(\mu)/\mu = [(um/m)^2 + (uD/D)^2 + (uL/L)^2]^{1/2}$. In the final analysis, the relative uncertainty of q is of the order of 5–6%. A comparison of $U\Delta T \approx 4.2$ °C with MAELOO = 7.23 °C and RMSELOO = 8.69 °C shows that the regression scatter reflects the combined effect of measurement uncertainty, geometry and technological differences between the samples.

Each experiment was carried out according to a single sequence: cooling the section to room temperature, filling with distilled water, vacuuming and sealing, recording the initial conditions, turning on the heater with a given power, recording the temperature series, fixing the quasi-stationary mode and cooling before the next experiment (Table 4).

2.6. Statistical Processing and Regression Model

To transition from the initial temperature series to the engineering model, standardized parameters were used: the lateral surface area of the bare section of the A_0, the specific electric heat load q and the specific mass of the μ [23,24,27].

$$q = \frac{P_{el}}{A_0}, \quad \mu = \frac{m}{A_0} \tag{14}$$

Local overheating of the upper zone of the section relative to the room temperature was set as [27]:

$$\Delta T = T_{final} - T_{room} \quad (15)$$

The extended regression model is based on the MP01–MP40 sample and has the form:

$$\Delta T = 118.42 + 0.05330q + 1.361V_{ml} - 11.097\mu \quad (16)$$

where ΔT—calculated overheating, °C; q—specific electric heat load of bare side surface, W/m^2; V_{ml}—working fluid volume, mL; μ—section specific gravity, kg/m^2. The coefficient of determination of the extended model, R^2fit = 0.911. Calculated local temperature is defined as [27]:

$$T_{calc} = T_{room} + \Delta T \quad (17)$$

Model quality was assessed by the coefficient of determination, mean absolute deviation, and standard error, including the leave-one-out test [27].

$$\begin{aligned} \mathrm{MAE} &= n^{-1}\sum_{i=1}^{n}\left|T_i - \hat{T}_i\right| \\ \mathrm{RMSE} &= \left[n^{-1}\sum_{i=1}^{n}\left(T_i - \hat{T}_i\right)^2\right]^{1/2} \end{aligned} \quad (18)$$

3. Results

3.1. External Heat-Transfer Limit of a Smooth Single Tube

The calculation of the external energy balance demonstrates the coordinated action of internal two-phase heat transfer and the external heat-dissipating surface. The evaporation–condensation mechanism equalizes the temperature field within the casing, whilst the power transferred to the room is determined by the surface area, the convection coefficient, the temperature level and the emissivity of the surface.

For a smooth tube with a diameter of 32 mm and a length of 340 mm, the effective lateral area is approximately 0.034 m^2. At a surface temperature of 90 °C, the calculated heat-transfer rate for this area ranges from 16.3 to 52.8 W, depending on h and ε. Design scenarios for a target power of 80 W are given in Table 5.

Table 5. External energy balance of a smooth single EVHP at Ts = 90 °C.

Estimated Case	h, W/(m^2·K)	ε	Q_{out} at $A_0 \approx 0.034$ m^2, W	A_{req} for 80 W, m^2	Conclusion
Natural convection, surface treated	6	0.50	24.1	0.114	It is recommended to increase the reduced surface to 0.114 m^2
Painted high-emission surface	6	0.90	31.8	0.086	The developed surface provides the target thickness at Areq = 0.086 m^2
Optimistic natural convection	8	0.50	28.8	0.095	Design area Areq = 0.095 m^2
Improved heat sink or developed surface	18	0.50	52.8	0.052	Intensive heat removal reduces the required area to 0.052 m^2
Control for bare copper	6	0.10	16.3	0.168	Lower limit of emissivity: Areq = 0.168 m^2

The obtained values indicate that the target power of 80 W corresponds to the full section or group of active elements. For its implementation, the reduced heat-emitting area is formed by finning, a jacket with a developed surface and, if necessary, combining several EVHP. This approach provides the required temperature level at a given power.

3.2. Numerical Comparison of Single-Phase and Two-Phase Modes

The control single-phase calculation shows that in the absence of an evaporation–condensation mechanism, the temperature maximum is localized in the heat supply zone. Along the height of the tube, a pronounced gradient occurs, which leads to overheating of the lower zone and incomplete use of the upper part of the surface (Figure 3).

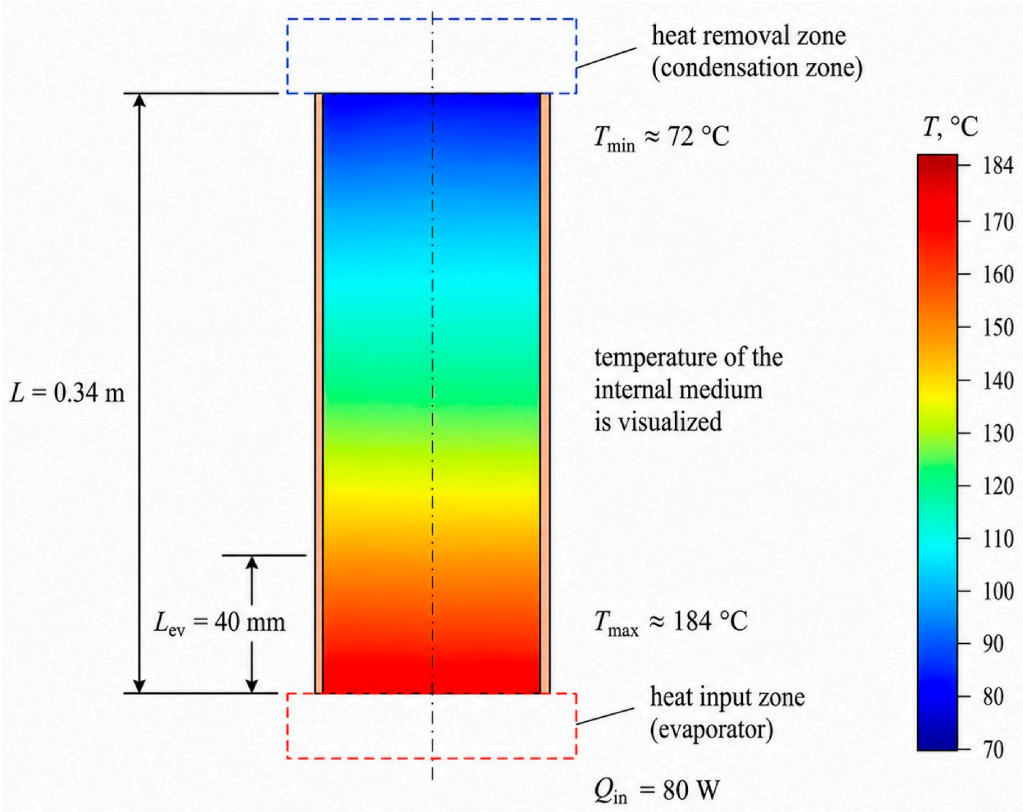


Figure 3. Temperature field in control single-phase mode with heat supply of 80 W.

The two-phase mode, on the contrary, demonstrates an almost uniform temperature field in height. This confirms the physical role of EVHP: it redistributes heat from the local electric heater to the condensation zone and side surface. At the same time, the average temperature level is still determined by the external balance considered in Section 3.1 (Figure 4).

Thus, numerical modeling confirms two different conclusions. The first conclusion: two-phase transfer really increases the uniformity of the temperature field. The second conclusion: the external heat-transfer area remains the main limiter of the permissible power at a given surface temperature.

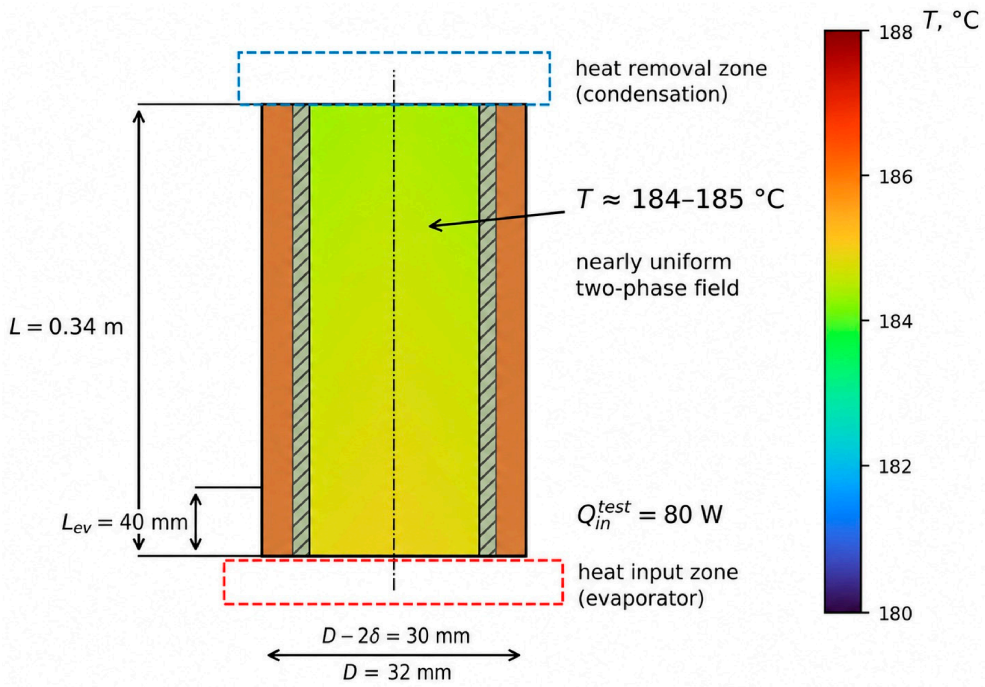


Figure 4. Temperature distribution in the test two-phase mode of a single EVHP with heat supply of 80 W.

The numerical model is verified by grid independence and energy balance. Experimental program MP01–MP40 was used for independent comparison of physical trends and engineering parameters. The sections closest to the calculated geometry with a diameter of 32 mm had a length of 350 mm (MP03, OP34, MP36) and worked at 60 and 100 W; their temperature responses are consistent with the identified role of specific load and two-phase heat redistribution.

3.3. Experimental Electrothermal Characteristics of the Section

The experimental program MP01–MP40 showed that the local temperature of the upper zone of the section varies in a wide range of 85.0–191.0 °C. This range refers to the laboratory bare tube, not the available surface of the finished instrument. In the finished LPSEH, the temperature of the accessible surface should be reduced by finning, casing, increasing the area and automatic regulation.

The average temperature of the upper zone in the main sample was 142.6 °C. At a rated power of 60 W, the average T_{final} value was about 130.9 °C; at 80 W—155.3 °C; at 100 W—160.8 °C. However, absolute power is not the only explanatory factor: different diameters, lengths, masses and volumes of the working fluid change the heat-transfer area and thermal inertia of the section.

The calculation of the local water–steam equilibrium condition relates the measured temperature levels to the saturation pressure: 142.6 °C corresponds to approximately 0.39 MPa, 155.3 °C—about 0.55 MPa, 191 °C—about 1.28 MPa. These values characterize the vapor component of pressure in forced laboratory modes and make it possible to quantitatively distinguish between the design range of 70–90 °C and the expanded area of experimental research.

The relationship between local overheating and the specific electrothermal load is shown in Figure 5. An increase in q is accompanied by an increase in ΔT, and the distribution of the experimental data points confirms the significance of the design and process factors included in the extended regression model.

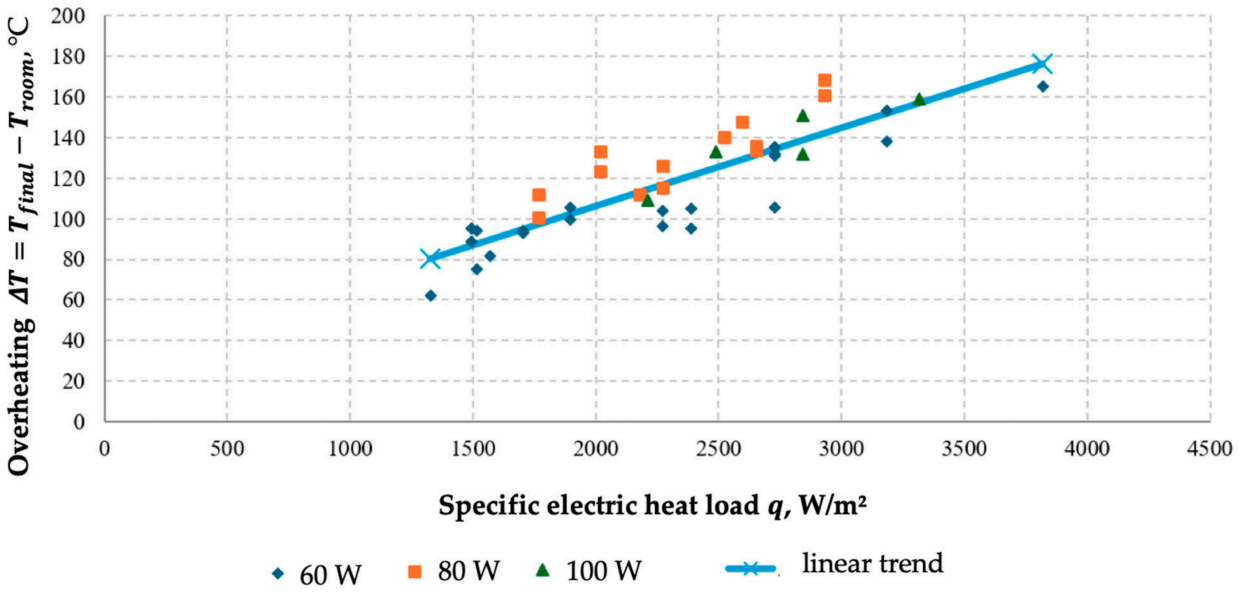


Figure 5. Dependence of local overheating of the upper section zone on specific electric heat load.

3.4. A Regression Model of Local Temperature Conditions

The basic extended model (16) takes into account three factors: specific electrothermal load q, working fluid volume V and specific mass μ. The sign of the coefficient at q is positive and reflects the increase in temperature with an increase in specific power (Table 6).

Table 6. Quality indicators of the temperature regression model.

Model	Factors	R^2_{fit}	R^2_{adj}	R^2_{LOO}	MAE_{LOO}, °C	$RMSE_{LOO}$, °C
Extended	q, V, μ	0.911	0.903	0.887	7.23	8.69
Abbreviated	q, μ	0.894	0.889	0.869	7.77	9.34

The coefficient at the working fluid volume is positive in the studied range of 10–15 mL. It should be interpreted as a technological amendment specifically for a given set of sections and modes, and not as a universal law for all degrees of filling. With a greater exit from the experimental area, a flood mode or deterioration of the steam space is possible.

The leave-one-out test shows that the average prediction error is in the range of 7–9 °C. For a laboratory thermal–technical model, this level is acceptable, since the spread includes the error of the temperature channel, differences in thermal contact, technological deviations in the manufacture of sections and the locality of the measurement point. At the same time, the model is not intended for direct prediction of the temperature of the casing of the finished device: it describes the internal laboratory section.

Equation (16) has been calibrated for the experimental range q = 1326–3820 W/m^2, V = 10–15 mL and μ = 10.04–14.96 kg/m^2. For the physically consistent boundary condition ΔT = 0 at q = 0, a model with forced passage through the origin has also been evaluated [27]:

$$\Delta T = q[0.05192 + 0.000593(V - 12.125) - 0.003969(\mu - 12.612)]. \quad (19)$$

For the model with a physical boundary condition, the following values were obtained: R^2fit = 0.905, R^2LOO = 0.888, MAELOO = 7.14 °C and RMSELOO = 8.64 °C. The comparability of the parameters of the two models confirms the robustness of the identified relationships and allows Equation (16) to be used as a local engineering regression within the experimental calibration range (Figures 6 and 7).

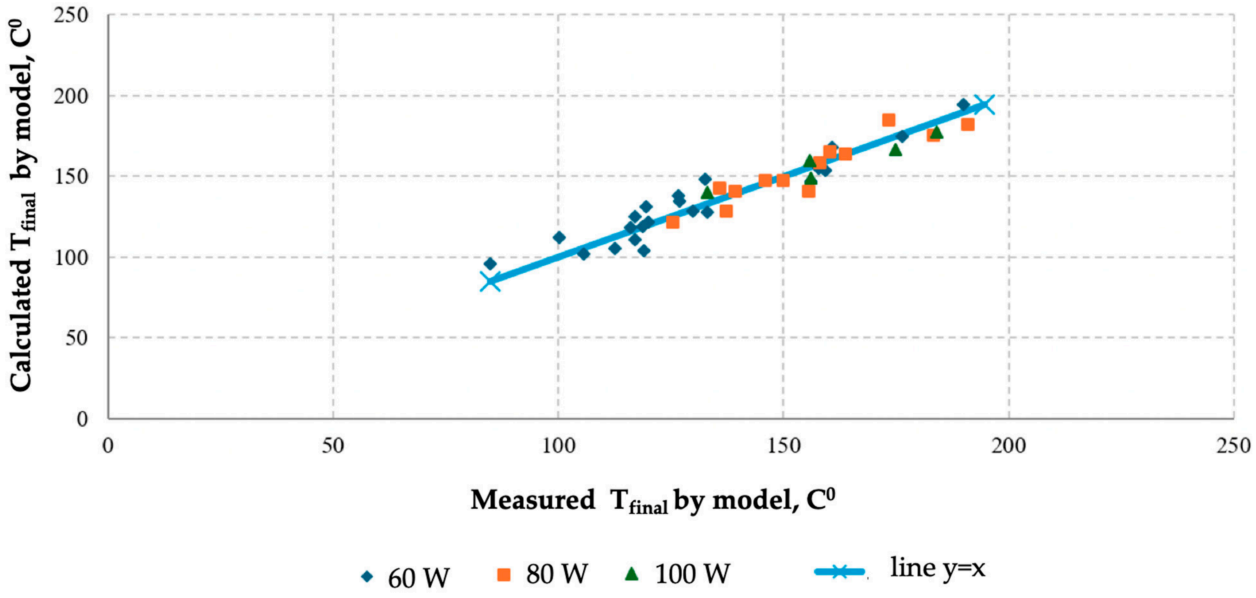


Figure 6. Comparison of measured and calculated temperature by regression model.

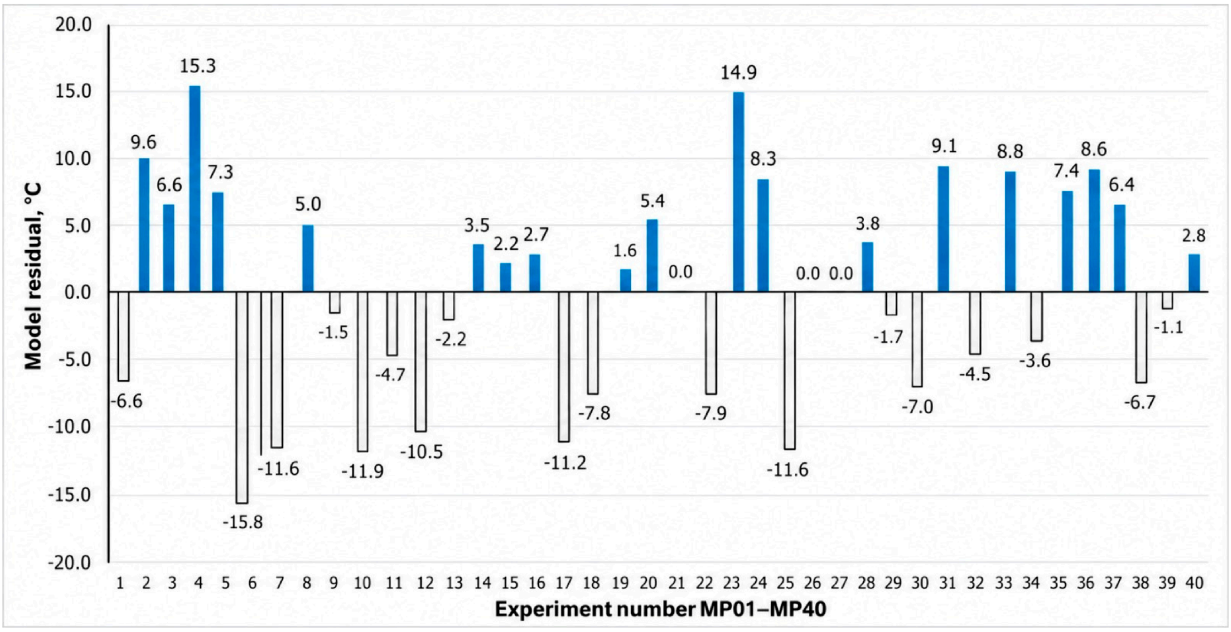


Figure 7. Regression model residuals for the MP01–MP40 series.

3.5. Effect of Initial Residual Pressure

The initial residual pressure affects the amount of non-condensable gases inside the sealed cavity. When heated, water steam displaces these gases into the upper region, where they may partially obstruct the condensation zone and alter the temperature response of the section.

In a specific comparison of similar configurations, the following results were obtained: for the MP39 series at P = 80 W, V = 10 mL, D = 28 mm, L = 40 cm, and p_0 = 9.807 kPa, the final temperature was T_{final} = 139.2 C; for the AP06 series, with the same basic parameters and p_0 = 5.066 kPa, T_{final} = 151.0 °C was obtained.

This series was not included in the main regression model, as the variation in p_0 requires a separate factorial design. However, the result is technologically significant: the

initial residual pressure must be controlled as a manufacturing parameter for EVHP, rather than being treated as a secondary operation.

In the comparison of MP39/AP06, the decrease in the initial residual pressure from 9.807 to 5.066 kPa was accompanied by an increase in the final local temperature of 11.8 °C. The identified trend highlights p_0 as a technologically significant parameter and justifies conducting an extended repeat series to quantify its contribution to the temperature regime.

3.6. Comparison of Tubular and Induction Heat Supply Methods

A separate experimental unit is devoted to comparing a tubular resistive heater THE-120 and an induction heater IDH-120 at the same active input power of 120 W (Table 7). The comparison was performed for the dynamic mode of reaching a local temperature of 200 °C (Figure 8).

Table 7. Comparison of tube and induction heat supply at P = 120 W.

Option	Heat Supply Type	*P*, W	T_{max}, °C	*t* Up to 200 °C, s	Energy Up to 200 °C, Wh	Interpretation
THE-120	resistive tubular	120	212	300	10.0	Basic version
IDH-120	induction HFT	120	247	180	6.0	Faster local heating

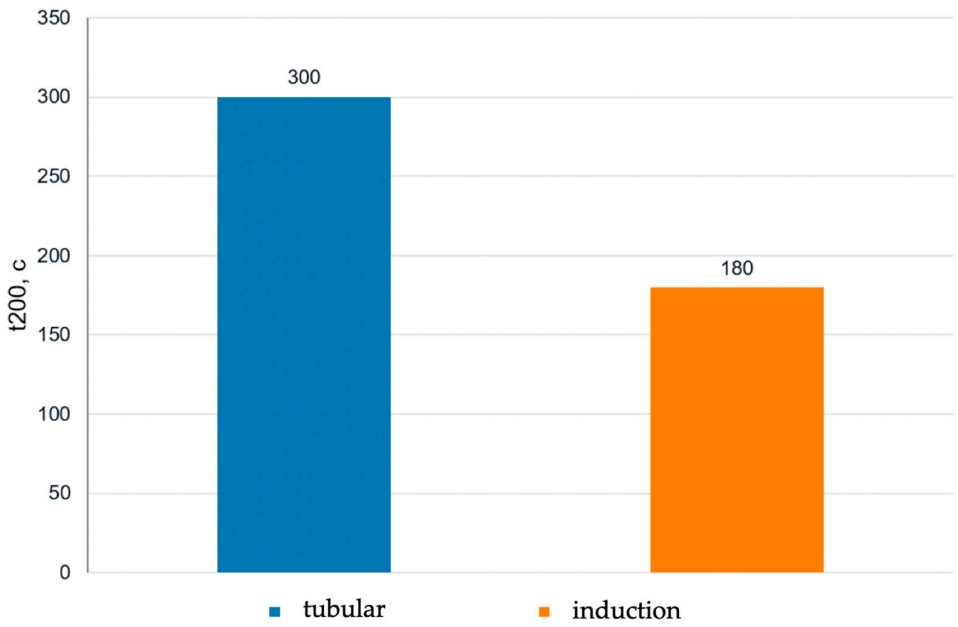


Figure 8. Time required to achieve a local temperature of 200 °C using tubular and induction heating.

The induction version reaches 200 °C in 180 s instead of 300 s; that is, it accelerates the achievement of the control temperature threshold by about 1.67 times. The energy expended to the reference level is reduced from 10.0 to 6.0 Wh.

3.7. Design Consequences for Sectional LPSEH

The total result of calculations and experiments forms the design criterion for the transition from a single EVHP to a sectional device (Table 8): the power of one section is selected jointly according to the capabilities of the heater, the stability of the internal phase transfer and the ability of the external surface to transmit the specified power at the design temperature [23–25].

$$\frac{P_i}{A_{reduced,i}} \le q_{\lim}(T_{s,\max}) \quad (20)$$

$$n_{\min} = \mathrm{ceil}\left(Q_{\text{target}}/Q_{\text{allow},1}\right) \quad (21)$$

where $A_{\text{reduced},i}$—the reduced available heat-emitting area of the i-th element, m^2; $q_{\lim}$—maximum specific heat transfer at the specified maximum surface temperature; $Q_{\text{allow},1}$—permissible heat transfer of one element; n_min is the minimum number of active elements.

Table 8. Engineering consequences of results for LPSEH design.

Established Result	Engineering Investigation
Two-phase mode equalizes the temperature by the height of the EVHP.	The EVHP is advantageously used as an internal heat-transfer assembly between the local heater and the distributed surface.
A smooth tube with a surface area of approximately 0.034 m^2 at 90 °C provides the baseline for external heat transfer.	Target power is realized by finning, casing with developed surface or a combination of several elements.
The regression model gives an error of the order of 7–9 °C.	The model is used for engineering selection of power and geometry in the studied area and forms the basis for verification of new line sizes.
The initial residual pressure affects the temperature reaction.	Evacuation is a process parameter of the section manufacturing quality.
Induction heat supply accelerates the output to the control temperature.	The induction version develops dynamic characteristics and provides for specialized electric power and EMC development.

3.8. Conceptual and Theoretical Foundations of a Generalized Non-Linear Physical and Mathematical Model of Processes in the Technological Device Under Investigation

Within the framework of this scientific paper, we used the general expression of the phenomenological model of thermodynamic and heat exchange processes on elements of a device such as an electric–vacuum heat pipe (EVHP) for a steam electric heating device (LPSEH), with a given design in the established experimental mode of operation of the device (temperature, pressure, density of steam and water; electric power of the heating device, etc.). This mathematical model is quite strict from the point of view of methods of technical thermodynamics and similarity theory in heat exchange processes, but incomplete and semi-empirical from the point of view of strict correspondence and synchronization of theoretical (calculated using the numerical calculation program using equations and formulas of the mathematical model) and measured (in laboratory or industrial tests) results and, to a large extent, depends on the data of the experiment, requiring regular adjustment of theoretical and experimental parameters during the performance of tests in real time. Even minor changes in operating characteristics (external connections to the device; energy loads of consumers or the environment; variable modes of operation of the device; malfunctions in the operation of the external electrical network feeding the device, etc.) lead, at the level of the proposed model, to noticeable deviations in the value and degree of synchronization of real (measured) results and those generated by the numerical calculation program (from the model equations). To increase the theoretical level, indicators of scientific originality of the mathematical model itself and indicators of its adaptability to the conditions of experiments, it is necessary to proceed to the development of a generalized nonlinear detailed physical and mathematical model of processes in the EVHP technological scheme for LPSEH in a wide range of varying numerical values of the

operating parameters and functions of the system (energy; thermal engineering; mechanical; geometric; information; system, etc.). The study of this generalized model is a separate scientific and technical problem and will be carried out in the future. Within the framework of this paper, we will limit ourselves to a conceptual description, preliminary quality assessments and schemes for further developments in this promising field of research, from the point of view of the interaction of the results of theory and experiment, direction of research.

Development of a generalized nonlinear physical and mathematical model of interrelated processes (thermodynamic; heat exchange; mass-transfer phenomena (in case of liquid evaporation and steam condensation) and temperature (in case of heat conductivity of electric heating device walls (wick) and heat pipe walls) in the process diagram of the LPSEH-based EVHP device), in the future, will be based on a verified (verified within the framework of the main provisions of this model) system of nonlinear equations in the form of differential equations of continuity of flows of matter (liquid; vapor) and energy (heat energy flux density with thermal conductivity and heat transfer) with the specified initial and boundary conditions specified for the processes of electrothermal and heat exchange energy transformations and mass energy transfer of flows in the EVHP scheme for LPSEH, in general, in order to prepare scientifically substantiated (within the methods of physical and technical thermodynamics and physical kinetics) theoretical schemes for algorithms of numerical detailed calculations for prediction of optimized process parameters in the EVHP model for the designed LPSEH. This model will work over a wide range of variation and measurement of each term—temperature, heat capacity and density of water vapor; steam thermal conductivity coefficient as a function of steam temperature; similar parameters for water; heat capacity and heat conductivity of heating device walls and heat tube walls—in the equations of the developed generalized model. In each individual energy equation, it is necessary to first clarify what is meant by the heat capacity (isobaric - typical for liquid working fluid, since the volume - respectively the heat capacity and density of the substance - of liquid (water) when heated to temperatures near boiling point and when cooled to temperatures near condensation temperature, near the point of phase transition of the first kind, changes significantly in time) or isochoric (in solid elements, when the volume -heat capacity and density- of the casing, in these temperature ranges does not change significantly during heating in the EVHP model for LPSEH. It is necessary to strictly designate and indicate, within the framework of the model of the energy process under consideration, in the EVHP model for LPSEH, on which thermodynamic and geometric parameters a single component value in the differential equation of energy and material transfer depends. For example, the heat capacity in the equation of thermal conductivity for a solid wall depends on the temperature (T), the density of the solid element, the thermal conductivity coefficient, and the local bulk density of the energy source should be considered, in the most generalized model, as a function of the radius vector of the spatial point, time, temperature, etc. It is very important, within the framework of a single or constructed equation of the energy process, to represent what each built-in parameter of the equation and the solution of the equation depend on. The description of each individual transport equation specified for this section (zone) of the technological process in the EVPH should be carried out on the basis of the known statistical and kinetic theory of a generalized nonlinear non-stationary equation of this type and, further, on its transformation into a partial differential equation (adapted to this particular mass energy transfer process) specifying new quotients (densities of flows of certain types of energy; volumetric densities of power sources, absorbers, etc.) adapted for this item of the proposed generalized model description plan. The preparation of the mathematical apparatus of this plan, in each of its points, will be built in such a way that, at the next step of solutions and development of

this analytical model, we can, according to a simplified version, by simple enumeration (based on a computer program), vary, with a high degree of accuracy and high speed, numerical data on system parameters and, on this basis, proceed to the implementation of virtual and real circuits of the EVHP device for LPSEH. Integral mathematical apparatus for EVHP-LPSEH should serve to implement this model as:

(1) Theoretical basis for the technological model and calculated numerical algorithms (differential equations; boundary and initial conditions for this system of equations; additional transformations).
(2) Physical model of the device (device) in the whole set of energy processes and transfer processes in the system.
(3) Bases for subsequent parametric identification of parameters and functions of the physical and mathematical model of the technological process.
(4) Methodological base for subsequent dimensionless analysis and optimization of these parameters and functionals of the system of transfer equations.
(5) The basis for the development of algorithms for numerical calculations and numerical optimization of the parameters of the experimental and technological scheme of the designed EVHP device for LPSEH. The main purpose of the developed (we will present in subsequent works) non-linear physical and mathematical model is to develop a comprehensive theoretical and computer-based (based on a package of numerical calculation programs) scheme of physical and numerical analysis and forecasting of technological schemes of a steam electric heating device based on an electric–vacuum heat pipe optimized for the requirements of the experiment and the production process.

Requirements for equations (and their additional conditions) of the developed physical and mathematical model of the device:

(1) Clear mathematical separation of local and global energy sources in a given element of the device design.
(2) Unified view of the surface and volume interpretation of phase transitions of the first kind in the system.
(3) Transition to enthalpy representation in energy equations in liquid and gaseous media (water; steam) in the zone of phase transitions of the first kind.
(4) Thermodynamic consistency of water and steam properties (according to state diagrams of the "water–steam" system).
(5) Strict unified representation of signs of projections of flow vectors (densities of energy flows; substance current density) at the boundaries of the device (system) elements.
(6) Application (construction) of a dimensionless parameter describing the share of energy losses in terms of the total useful energy of the flow at a given element of the device (energy loss coefficient).
(7) Formation of a single verified system of nonlinear equations describing the processes on the elements of EVHP for LPSEH.

The study of the complete closed systems of nonlinear nonstationary differential equations of the physical and mathematical model for the process diagram of the EVHP device of the LPSEH type will be based on a methodology based on a consistent and complex justification of equations, analysis of nonlinear properties and solutions of (analytical; numerical) differential equations of mass and energy transfer in the process system:

(1) The unsteady distribution of steam density and its spatial transfer in the cavity of the heat pipe, with the generation of steam at the source and its condensation on the condensation part of the system, will be described on the basis of the continuity equation for this process [9,68–72], with refinements (originality elements) on the right

side of the equation (in mathematical modeling of the flow rates of matter during evaporation and condensation). In [68,70,72] there are given fundamental principles of construction of equations of conservation of mass, momentum and energy, as well as a description of mechanisms of convection, diffusion and heat-conducting energy transfer in systems. The methodology from [68,72–76] will be used as a basic theoretical justification for the local differential equations of the EVHP model and their relationship to general conservation laws and their interpretations.

(2) The redistribution of water in the system, including the evaporation process, condensation and water return through the wick, will be described by the continuity equation for the total mass of water in the system [2], by mathematical modeling of the relationships between changes over time in the amount of liquid water in the source (element), in the evaporation zone (on the condensation device) and during capillary water supply in the wick. In [9,69–78], fundamental schemes for physical and mathematical modeling of heat tube technologies are proposed: analytical models of heat-transfer processes in solid–liquid-vapor systems, liquid capillary movement, evaporation and condensation, interphase heat transfer and mass transfer, hydrodynamic movements of steam and liquid, stationary and transient modes, heat-transfer limitations and operation of two-phase thermosyphons are described. When developing a generalized nonlinear EVHP model, the originality of the mathematical model will be based on the formation of the right-hand side of the differential equation (when modeling the kinetics of the processes of evaporation and condensation of the liquid phase of the working substance, and the description of capillary processes). Electrothermal effects associated with heating of the coolant (liquid water) and its evaporation under the action of the heater should be carried out, with a strict theoretical approach, in conjunction with the equation of continuity of electric charge and the Poisson equation for the electric potential in the structure of the heating element, taking into account the characteristics of the source of external electric voltage (EMF circuit). The process of thermal conductivity in the wall of the heating device, which ensures the transfer of thermal energy from the electric heating element to the working zone of the EVHP (to liquid water), should be carried out on the basis of a generalized nonlinear differential equation of thermal conductivity for this wall under the initial and boundary conditions determined in the model. The originality of the approach will be the development of a universal model and a generalized non-linear equation of thermal conductivity in dimensionless variables (dimensionless time and dimensionless coordinates of points inside the wall) to describe space-time temperature distributions in the element (heating device wall) of arbitrary geometric shape and symmetry, with an arbitrary distribution law (bulk density) of energy in a local source, taking into account diffusion nonlinear effects caused by intense phonon–phonon interaction in the element structure (spatially inhomogeneous non-stationary thermal conductivity coefficient in Fourier's law) [19,79,80].

An investigation into the properties of the generalized non-linear, non-stationary energy transformation equation governing the gas-phase flow of the working fluid (water vapor) in the modeled EVHP (hereinafter, simply the steam energy equation) will be carried out on the basis of the closed-loop nature of the steam flow within the system (in the energy representation), taking into account all the driving forces associated with steam formation processes (heating and evaporation of the liquid; generation and condensation of steam) and the internal thermodynamic properties of the steam as a continuous hydrodynamic flow. We shall rely on the law of conservation of energy in the $\frac{dW_v}{dt} = 0$ for the steam subsystem. We present the total energy of the simulated system (vapor-phase water, vapor water) with volume V in the form of $W_v(t) = \oint_V W_{vV}\left(\vec{r};t\right)dV$. Applying to the

spatially inhomogeneous, non-stationary function of the system (vapor water) $W_{vV}\left(\vec{r};t\right)$ the enthalpy representation $W_{vV}\left(\vec{r};t\right) = \rho_v\left(\vec{r};t\right)c_p(T) \times T$ from the theorem known from differential geometry, we have a fundamental energy equation for the flow of water vapor in the system (device of the EVHP type), applicable to other similar in nature physical processes and technological systems:

$$\frac{dW_v}{dt} = \oint_V \left(\frac{\partial W_{vV}\left(\vec{r};t\right)}{\partial t} + \vec{\nabla}\left(E_{vV}\left(\vec{r};t\right)\vec{u}\right) \right) dV = -\oint_S \vec{q}_{ext,v}\vec{dS} \tag{22}$$

We simulate the volumetric density of the total energy of the steam flow in the $E_{vS}(t)$ system in the form:

$$E_{vV}\left(\vec{r};t\right) = \frac{dE_{vS}(t)}{dV} = \rho_v\left(\vec{r};t\right)E_v\left(\vec{r};t\right) \tag{23}$$

The specific total energy $E_v\left(\vec{r};t\right) = \frac{dE_{vS}(t)}{dm_v}$ of the hydrodynamic flow of steam in the system $E_v\left(\vec{r};t\right) = \frac{\vec{u}^2}{2} + \frac{p_v\left(\vec{r};t\right)}{\rho_v\left(\vec{r};t\right)} + u_{Tv}$ is made up of the specific values, respectively, of the kinetic energy of the flow $E_{vK}\left(\vec{r};t\right) = \frac{\vec{u}^2}{2}$, the potential energy (expressed in terms of steam pressure), as measures of the internal force effect of the flow $E_{vP}\left(\vec{r};t\right) = \frac{p_v\left(\vec{r};t\right)}{\rho_v\left(\vec{r};t\right)}$, the internal (thermal) energy of the flow of water vapor $u_{Tv} = \rho_v\left(\vec{r};t\right)c_V(T) \times T$. Let us consider the pressure in the system as a function:

$$p_v\left(\vec{r};t\right) = p_{Tv}(T) + p_{\Gamma v}(T) - \tau_{nv}\left(\vec{r};t\right) + \rho_v\left(\vec{r};t\right)gz \tag{24}$$

where $p_{\Gamma v}(T)$—piezometric (power) vapor pressure, $\tau_{nv}\left(\vec{r};t\right)$—viscous internal stress of vapor medium, $\rho_v\left(\vec{r};t\right)gz$—hydrostatic vapor pressure.

The energy flux density vector in the simulated system (water vapor) $\vec{q}_v\left(\vec{r};t\right) = \rho_v\left(\vec{r};t\right)E_v\left(\vec{r};t\right)\vec{u}$ reflects the influence of all power and thermodynamic factors allowed in the system on the properties and parameters of the hydrodynamic vapor flux, including the most general form of Fourier's law for thermal conductivity $\vec{q}_T\left(\vec{r};t\right) = -\vec{\nabla}\left(\chi_v\left(\vec{r};t\right)T\left(\vec{r};t\right)\right)$, where $\chi_v\left(\vec{r};t\right)$ is the generalized spatially inhomogeneous non-stationary coefficient of diffusion of water vapor. Then,

$$\vec{q}_v\left(\vec{r};t\right) = W_{vV}\left(\vec{r};t\right)\vec{u}_v + \left(p_{\Gamma v}(T) - \tau_{nv}\left(\vec{r};t\right) + \rho_v\left(\vec{r};t\right)gz\right)\vec{u}_v - \vec{\nabla}\left(\chi_v\left(\vec{r};t\right)T\left(\vec{r};t\right)\right) \tag{25}$$

Modeling the right side of the main equation $N_{ext} = \oint_S \vec{q}_{ext,v}\vec{dS} = \int_V div\,\vec{q}_{ext,v}dV$, as the system power associated with heat exchange processes (convection, thermal conductivity) and phase transitions of the first kind (evaporation of liquid water to the state of steam; condensation of steam to the state of liquid), we take the kinetic component of the volumetric density of the flow power (kinetic power of a unit of the flow volume) of vapor (in the working substance phase conversion zone on the elements where the liquid evaporates (evaporator), and the steam condenses (on the inner wall of the heat pipe) respectively) in the form of:

$$q_{ext,v,V}\left(\vec{r};t\right) \equiv -div\,\vec{q}_{ext,v,V} = S_{ev,pc} + q_{w\longrightarrow v,V} \tag{26}$$

The value of $S_{ev,pc} = (\Gamma_{ev} - \Gamma_{cond})h_{v,i}$ can be interpreted as an increment of the volumetric density of water vapor power at the interface of two phases, and the $h_{v,i} = h_v$ parameter as the specific enthalpy of the water vapor at the interface. Determination of power bulk density jump in $S_{ev,pc} = \Gamma_{ev,cond}h_v$ format is a conservative calculation scheme for this parameter. The updated latent heat calculation scheme takes into account the specific enthalpy of liquid water h_l at the interface of two phases $S_{ev,pc} = \Gamma_{ev,cond}L_{v,l}$, where $\Gamma_{ev,cond} = \Gamma_{ev} - \Gamma_{cond}$ has $\frac{\text{kg}}{\text{m}^3\cdot\text{s}}$ dimension of substance flow rate by mass per unit time), where the parameter Γ_{ev} describes the process of water evaporation in the evaporator zone (evaporator zone) and depends on the thermodynamic parameters of steam and water in this area, and the Γ_{cond} parameter accordingly describes the process of condensation of vapor in the vapor condensation zone; $L_{v,l} = h_v - h_l$ is the latent heat of vaporization. Latent scheme of $S_{ev,pc}$ parameter calculation is effective for engineering calculations and requires strict observance of signs in this expression. The conservative expression is effective in fundamental thermophysical research and qualitatively consistent with the laws of conservation of energy and mass. The kinetic power density component $q_{w\longrightarrow v,\text{V}}$ is responsible for the heat exchange process between the inner wall of the heat pipe and water vapor and has the form $q_{w\longrightarrow v,\text{V}} = (\text{T}_w - \text{T}_v)a_{v,w}\alpha_{v,w}$, where $\alpha_{v,w}$ is the heat-transfer coefficient at the boundary between the wall and vapor flow $\left(\frac{\text{W}}{\text{m}^2\cdot\text{K}}\right)$. $\alpha_{v,w}$ is a clarifying parameter for the volume distribution of the heat-transfer process, measured in reverse meters.

The generalized nonlinear differential energy equation for water vapor (taking into account phase transitions and heat exchange processes in the EVHP device) takes the form

$$\begin{aligned}\frac{\partial\left(\rho_v\left(\vec{r};t\right)c_p(\text{T})\times\text{T}\right)}{\partial t} + \vec{\nabla}\left(\rho_v\left(\vec{r};t\right)c(\text{T})\times\text{T}\vec{u}_v\right) + \vec{\nabla}\left(\left(p_{\Gamma v}(\text{T}) - \tau_{nv}\left(\vec{r};t\right) + \rho_v\left(\vec{r};t\right)gz\right)\vec{u}_v\right) - \\ \vec{\nabla}\left(\chi_v\left(\vec{r};t\right)\vec{\nabla}\text{T}\left(\vec{r};t\right)\right) + (\Gamma_{ev}(\text{T}) - \Gamma_{cond}(\text{T}))L_{v,l}(\text{T}) + (\text{T}_w - \text{T})a_{v,w}(\text{T})\alpha_{v,w}(\text{T})\end{aligned} \quad (27)$$

This equation is generally solved in conjunction with the mass continuity equation for water vapor

$$\frac{\partial\rho_v\left(\vec{r};t\right)}{\partial t} + \vec{\nabla}\left(\rho_v\left(\vec{r};t\right)\vec{u}_v\right) = \Gamma_{ev}\left(\vec{r};t\right) - \Gamma_{cond}\left(\vec{r};t\right) \quad (28)$$

and the Navier–Stokes-Fourier momentum equation for water vapor flow in the system

$$\frac{\partial\left(\rho_v\left(\vec{r};t\right)\vec{u}_v\right)}{\partial t} + \vec{u}_v\cdot\vec{\nabla}\left(\rho_v\left(\vec{r};t\right)\times\vec{u}_v\right) = -\vec{\nabla}\left(p_{\Gamma v}(\text{T}) - \tau_{nv}\left(\vec{r};t\right) + \rho_v\left(\vec{r};t\right)gz\right) + \left(\Gamma_{ev}\left(\vec{r};t\right) - \Gamma_{cond}\left(\vec{r};t\right)\right)\vec{u}_v \quad (29)$$

The proposed system of water vapor equations is nonlinear, non-stationary, and closed for the whole physical system, which is consistent with the technological scheme of the device, which indicates the necessity to write a similar system of equations for liquid water and a nonlinear general equation of heat conductivity for mathematical interpretations of heat-transfer processes in solid-state elements of EVHP structure for LPSEH. Continuation of records, analysis of properties and construction of original closed nonlinear systems of equations for processes of energy exchange, mass transfer and equations of hydrodynamics of flows of working substances in the system of EVHP type shall be disregarded in subsequent works. In this scientific article, we limited ourselves to an example of a preliminary phenomenological assessment of non-linearities and the structure of the thermomechanical energy equation for the flow of water vapor in the EVHP. Analytical constructions and estimates of kinetic parameters of the energy equation responsible for the processes of steam heat exchange with system elements and phase transitions in the EVHP design were performed.

When developing analytical solutions to equations of this type, methods and computational schemes similar to those described in [81–84] will be employed. Although the physical nature and technological conditions of the processes investigated by the authors in [81–84] differ fundamentally from those considered in this study—namely, electrophysical phenomena associated with ion transport in an electric field within layered dielectrics versus the transfer of mass, energy, and momentum of the working fluid during phase transitions in the water-vapor system of the EVHP—the mathematical foundations of the corresponding systems of differential equations and the approaches used to solve these nonlinear physical and mathematical models are largely similar. In both cases, the models are governed by interrelated material properties, structural parameters, and methods for analyzing their thermal and mass-transfer behavior.

4. Discussion

The obtained results characterize EVHP LPSEH as a bound electrothermal and two-phase object. Internal evaporation–condensation transfer increases the uniformity of heat distribution in height, and the level of external heat transfer is determined by surface area, temperature, convection and radiation. Therefore, rational design of LPSEH combines the choice of heater with the calculation of the reduced heat-emitting surface.

The identified patterns are consistent with the independent literature on heat pipes and thermosyphons [5–14,33,34]. Works [15,16,18,28–32] document the sequence of development of specific EVHP/LPSEH and supplement the general theoretical base with the results of previously tested structures.

The principal difference in the proposed installation is the separate consideration of the active power of the heater and the ability of a particular external surface to transmit this power to the room. For a fully housed electrical appliance, all consumed active power is ultimately converted to heat, and the temperature of the accessible surface is determined by the area and intensity of external heat exchange.

The sensitive calculation of Table 4 gives, for a smooth tube at Ts ≈ 90 °C, the range Q_{out} = 16.3–52.8 W and the required reduced area A_{req} = 0.052–0.168 m^2. The narrower values of 24.1–31.8 W and 0.086–0.114 m^2 refer only to two basic scenarios with h = 6 W/(m^2·K) and different emissivity. Therefore, it is the full range that is used in formulating the uncertainty of the design estimate.

A comprehensive interpretation of the results is based on three complementary levels. The first level involves a scenario-based calculation of the external heat transfer from a smooth tube across a range of h and ε. The second involves numerical verification of COMSOL with regard to mesh stability and energy balance. The third is the experimental identification of temperature dependencies and a regression model based on 40 runs (MP01–MP40). At Ts = 90 °C, the calculated heat transfer Q_{out} = 16.3–52.8 W corresponds to 20–66 per cent of the target power of 80 W; the calculated equivalent area required to achieve this is 0.052–0.168 m^2.

Comparison with the independent literature confirms the consistency of the trends identified. A review of heating systems with heat pipes [12] identifies the source temperature, orientation, working fluid and filling factor as the main factors of thermal efficiency. In the experimental study of gravitational heat pipes [13] at capacities of 40, 60 and 80 W, the sensitivity of thermal characteristics was ranked as input power > filling factor > pipe configuration, which qualitatively agrees with the positive effect of the specific load q and the significance of the working fluid volume V in this sample. Work [14] confirms the effectiveness of the joint use of CFD and experiment for the study of closed thermosyphons, and the results for heating terminals [34] are consistent with the approach of joint design of a heat pipe and a developed radiator surface.

The scaling of the results of laboratory EVHP to the instrument level is carried out through the design criteria for specific load, reduced area, degree of filling and stable condensate return. In the extended instrument program, the LPSEH-500 sample with the same active power of 500 W reached a surface temperature of 90 °C in 119 s versus 593 s for the control oil heater; the output energy at this level was 16.5 and 82.4 Wh, respectively. In the construction series, the use of a drainage channel and finning reduced the maximum temperature difference between the control zones from 27 to 34 to 6–7 °C. These results confirm the applicability of the stated principles of transition from a single EVHP to a sectional instrument module.

The regression model relates the electrical mode and design parameters of the section to the local temperature of the upper zone. The positive coefficient at q is consistent with the external thermal balance, and the negative coefficient at μ reflects the influence of structural mass and thermal inertia. The model is calibrated at the MP01–MP40 range and forms the basis for subsequent parametric verification of new lengths, diameters, materials, degrees of filling and surface options.

An additional model (19) satisfying $\Delta T(q = 0) = 0$ demonstrates comparable predictive ability and provides physically consistent boundary behavior at zero power. The coincidence of the quality indicators of the two models confirms the stability of the identified relationships within the experimental range.

Comparison of MP39/AP06 shows a pronounced temperature sensitivity to the initial residual pressure and the content of non-condensable gases. On this basis, p_0 is isolated as a technological parameter of vacuuming and as an independent factor for an extended repeated series focused on the quantitative identification of its contribution to the temperature regime.

Comparison of tubular and induction heaters shows the advantage of induction supply in terms of local heating dynamics. For instrument applications, thermal dynamics is considered in conjunction with power factor, current harmonic composition, transducer efficiency, electromagnetic compatibility, power part reliability, and cost. The resistive sectional version forms the basic instrument configuration, and the induction version represents a promising direction for increasing dynamic characteristics.

The range of applicability of the obtained results covers laboratory EVHP and the design transition to the sectional instrument module. The extended temperature range of 85–191 °C characterizes the internal sections, while the temperature of the accessible surface is set by finning, casing and the control algorithm. Further experimental program provides for recording of operating pressure, study of hydrodynamic limits, repeated factor analysis p_0, tests at degraded convection, cyclic modes and long-term leak test. Such a complex provides a consistent transition from a thermophysical model to a verified instrument structure.

5. Conclusions

1. LPSEH electric–vacuum heat pipe is physically justified as a wickless closed gravity two-phase thermosiphon, in which active electric power is supplied to the evaporation zone, and heat is transferred to the condensation zone due to the phase transition of the working fluid.
2. The proposed power plant separates active electric power, heat power in the evaporation zone and useful heat transfer of the selected external surface. This separation ensures the correct calculation of the temperature regime, heat-transfer area and section power while maintaining the overall energy balance of the electric heater.
3. The calculation of the external convection–radiation balance showed that for a smooth tube with a diameter of 32 mm and a length of 340 mm at Ts = 90 °C in the considered

range of h and ε, the calculated heat transfer is 16.3–52.8 W, and a reduced area of 0.052–0.168 m^2 is required for 80 W removal. The values of 24.1–31.8 W and 0.086–0.114 m^2 correspond to the basic scenarios at h = 6 W/(m^2·K).

Q_{out} and A_{req} parameters characterize the calculated design range of external heat transfer, formed by the h and ε values; the experimental program complements it with quantitative temperature responses of sections and a statistical model of local mode.

4. Numerical modeling confirmed the qualitative difference between single-phase and two-phase modes. When phase transfer is disabled, the temperature is localized near the heat supply zone; in two-phase mode, the temperature field along the height of the tube becomes significantly more uniform.

   The numerical model is verified by grid stability and energy balance, and the experimental program provides independent confirmation of key physical trends: the influence of specific load, geometry, working fluid volume and two-phase heat redistribution.
5. Based on experimental data MP01–MP40, an engineering regression model of local overheating of the upper zone of the section was obtained: $\Delta T = 118.42 + 0.05330q + 1.361V_{ml} - 11.097\mu$. For the model, R^2_{fit} = 0.911, R^2_{adj} = 0.903, R^2_{LOO} = 0.887, MAE_{LOO} = 7.23 °C and $RMSE_{LOO}$ = 8.69 °C.

   Model (16) is calibrated for the experimental range q = 1326–3820 W/m^2, V = 10–15 mL and μ = 10.04–14.96 kg/m^2; an additional model (19) with the condition ΔT (q = 0) = 0 gives R^2 LOO = 0.888, MAELOO = 7.14 °C and RMSELOO = 8.64 °C, confirming the stability of the regression relationships.
6. Compared with MP39/AP06, a decrease in the initial residual pressure from 9.807 to 5.066 kPa was accompanied by an increase of 11.8 °C in the final local temperature. The result highlights p_0 as a significant process parameter of vacuuming and forms the basis for its quantitative identification in the extended factor series.
7. An induction heat input of 120 W accelerated the local temperature of 200 °C from 300 to 180 s and reduced the energy required to reach the control threshold from 10.0 to 6.0 Wh. The instrument implementation of the induction version includes a specialized high-frequency converter, power factor correction and electromagnetic compatibility.
8. The obtained results set engineering conditions for the transition from a single EVHT to a sectional instrument module: development of a heat-emitting surface, rational choice of specific heat load, technological control of vacuuming, stable condensate return and temperature control when scaling the structure.

Supplementary Materials: The following supporting information can be downloaded at: https://www.mdpi.com/article/10.3390/app16199464/s1. Table S1. Complete matrix of the main experimental program OP01–OP40, used to calculate group means and the regression model.

Author Contributions: Conceptualization, R.B., A.M. and V.K.; methodology, R.B., A.M., Y.N. and V.K.; software, A.M.; validation, R.B., A.M., Y.N., V.K. and O.A.; formal analysis, R.B., A.M., Y.N., V.K. and O.A.; investigation, R.B., A.M., Y.N., V.K. and O.A.; resources, A.M. and Y.N.; data curation, A.M., Y.N. and V.K.; writing—original draft preparation, R.B., Y.N. and V.K.; writing—review and editing, A.M., Y.N. and V.K.; visualization, R.B. and O.A., supervision A.M.; project administration, A.M. and Y.N.; funding acquisition, A.M. All authors have read and agreed to the published version of the manuscript.

Funding: This research was funded by the Science Committee of the Ministry of Science and Higher Education of the Republic of Kazakhstan under the project AP25795573 "Development of an energy-efficient steam electric vacuum heater for domestic and industrial heating".

Institutional Review Board Statement: Not applicable.

Informed Consent Statement: Not applicable.

Data Availability Statement: The original contributions presented in this study are included in the article. Further inquiries can be directed to the corresponding authors.

Conflicts of Interest: The authors declare no conflicts of interest.

Abbreviations

The following abbreviations are used in this manuscript:

EVHP	Electric vacuum heat pipe
LPSEH	Low-pressure steam electric heater
EHD	Electrical heating devices
MP	Main program
AP	Additional program
IDH	Induction heater
THE	Tubular electronic heater
HFT	High-frequency transducer
EMC	Electromagnetic compatibility

References

1. On Approval of the National Development Plan of the Republic of Kazakhstan Until 2029. Decree of the President of the Republic of Kazakhstan No. 611, 30 July 2024. Available online: https://www.refworld.org/legal/decreees/natlegbod/2024/ru/151293 (accessed on 9 August 2026).
2. On Energy Saving and Energy Efficiency. Law of the Republic of Kazakhstan No. 541-IV, 13 January 2012. Available online: https://policy.asiapacificenergy.org/node/135 (accessed on 9 August 2026).
3. Bloess, A.; Schill, W.-P.; Zerrahn, A. Power-to-heat for renewable energy integration: A review of technologies, modeling approaches, and flexibility potentials. *Appl. Energy* **2018**, *212*, 1611–1626. [CrossRef]
4. Maruf, M.N.I.; Morales-España, G.; Sijm, J.; Helistö, N.; Kiviluoma, J. Classification, potential role, and modeling of power-to-heat and thermal energy storage in energy systems: A review. *Sustain. Energy Technol. Assess.* **2022**, *53*, 102553. [CrossRef]
5. Jouhara, H.; Chauhan, A.; Nannou, T.; Almahmoud, S.; Delpech, B.; Wrobel, L.C. Heat pipe based systems—Advances and applications. *Energy* **2017**, *128*, 729–754. [CrossRef]
6. Dan, P.D.; Ray, D.A. *Heat Pipes*; Energiya: Moscow, Russia, 1979; 272p.
7. Chi, S. *Heat Pipes: Theory and Practice*; Mashinostroenie: Moscow, Russia, 1981; 207p.
8. Bezrodny, M.K.; Pioro, I.L.; Kostyuk, T.O. *Transfer Processes in Two-Phase Thermosyphon Systems*; Fakt: Kyiv, Ukraine, 2005; 704p.
9. Faghri, A. *Heat Pipe Science and Technology*; Taylor & Francis: Washington, DC, USA, 1995; 874p.
10. Abdullahi, B.; Al-dadah, R.K.; Mahmoud, S. Thermosyphon Heat Pipe Technology. In *Recent Advances in Heat Pipes*; IntechOpen: London, UK, 2019.
11. Maghrabie, H.M.; Olabi, A.; Alami, A.H.; Al Radi, M.; Zwayyed, F.; Salamah, T.; Wilberforce, T.; Abdelkareem, M.A. Numerical simulation of heat pipes in different applications. *Int. J. Thermofluids* **2022**, *16*, 100199. [CrossRef]
12. Dong, S.; Chen, J.; Lv, C.; Yuan, T.; Liu, Y.; Huang, X.; Liu, Z. A review of the building heating system integrated with the heat pipe. *Processes* **2024**, *12*, 2218. [CrossRef]
13. Lu, X.; Liu, J.; Tong, X.; Dai, R.; Xiao, Y.; Deng, J. Experimental investigation on thermal performance of gravity heat pipe with different pipe configurations. *Case Stud. Therm. Eng.* **2025**, *65*, 105695. [CrossRef]
14. Ritthong, N.; Thongkom, S.; Sawisit, A.; Duangsa, B.; Ritthong, W. Optimization design of closed-loop thermosyphons: Experimentation and computational fluid dynamics modeling. *Energies* **2024**, *17*, 527. [CrossRef]
15. Mekhtiyev, A.D.; Kim, P.M.; Yugay, V.V.; Alkina, A.D. Electrovacuum heating elements. *Bull. Karaganda Univ. Phys. Ser.* **2019**, *3*, 27–33. [CrossRef]
16. Mekhtiyev, A.D.; Kim, P.M.; Yugay, V.V.; Alkina, A.D. Heating radiator with vacuum tubes. Kazakhstan Utility Model Patent No. 4219, 1 August 2019.
17. Karpenko, A.N.; Shchukin, A.B. Electric heater of steam-drop type. Russian Federation Utility Model Patent RU 186444 U1, 21 January 2019.
18. Mekhtiyev, A.; Breido, I.; Buzyakov, R.; Neshina, Y.; Alkina, A. Development of low-pressure electric steam heater. *East.-Eur. J. Enterp. Technol.* **2021**, *4*, 34–44. [CrossRef]

19. International Association for the Properties of Water and Steam (IAPWS). *Revised Release on the IAPWS Industrial Formulation 1997 for the Thermodynamic Properties of Water and Steam (IAPWS R7-97(2012))*; IAPWS: Lucerne, Switzerland, 2012.
20. COMSOL AB. *Heat Transfer Module User's Guide, version 6.4*; COMSOL AB: Stockholm, Sweden, 2025.
21. COMSOL AB. *CFD Module User's Guide, version 6.4*; COMSOL AB: Stockholm, Sweden, 2025.
22. COMSOL AB. *Porous Media Flow Module User's Guide, version 6.4*; COMSOL AB: Stockholm, Sweden, 2025.
23. Dulnev, G.N. *Theory of Heat and Mass Transfer*; Saint Petersburg National Research University of Information Technologies, Mechanics and Optics (ITMO): Saint Petersburg, Russia, 2012; 195p.
24. Fokin, V.M.; Boykov, G.P.; Vidin, Y.V. *Fundamentals of Energy Saving in Heat Exchange*; Mashinostroenie-1: Moscow, Russia, 2005; 192p.
25. *GOST IEC 60335-2-30-2013*; Safety of Household and Similar Electrical Appliances—Part 2-30: Particular Requirements for Room Heaters. Interstate Council for Standardization, Metrology and Certification: Minsk, Belarus, 2013.
26. *ST RK 2.87-2005*; State System for Ensuring the Uniformity of Measurements of the Republic of Kazakhstan. Thermocouples. Nominal Static Characteristics of Transformation. Committee for Technical Regulation and Metrology: Astana, Kazakhstan, 2005.
27. *GOST 34100.3-2017/ISO/IEC Guide 98-3:2008*; Measurement Uncertainty—Part 3: Guide to the Expression of Uncertainty in Measurement (GUM). Interstate Council for Standardization, Metrology and Certification: Minsk, Belarus, 2017.
28. Mekhtiyev, A.D.; Buzyakov, R.R.; Kim, P.M.; Alkina, A.D. Study of the parameters of the induction vacuum heater of the low-pressure steam electric heater. *Proc. Univ.* **2021**, *3*, 262–267. [CrossRef]
29. Mekhtiyev, A.D.; Buzyakov, R.R.; Shapenova, Z.R. Low-pressure steam electric heater. *Vestn. Toraighyrov Univ. Energy Ser.* **2022**, *3*, 123–134.
30. Mekhtiyev, A.D.; Buzyakov, R.R. A low-pressure steam electric heater as the basis of a new generation autonomous heating system. *Bull. KazATC* **2023**, *5*, 474–481. [CrossRef]
31. Buzyakov, R.R.; Mekhtiyev, A.D.; Neshina, Y.G.; Alkina, A.D.; Bilichenko, A.P. Studying characteristics of the heat pipe of a low-pressure steam electric heater with different types of heaters. *Eurasian Phys. Tech. J.* **2025**, *22*, 46–52. [CrossRef] [PubMed]
32. Buzyakov, R.; Mekhtiyev, A.; Yurchenko, A.; Alpysbayeva, N.; Bilichenko, A. Efficiency of the building heating system with the use of low-pressure steam electric heaters. *Proc. Univ.* **2025**, *4*, 435–441. [CrossRef]
33. Kılkış, B.; Çağlar, M.; Şengül, M. Energy benefits of heat pipe technology for achieving 100% renewable heating and cooling for fifth-generation low-temperature district heating systems. *Energies* **2021**, *14*, 5398. [CrossRef]
34. Kerrigan, K.; Jouhara, H.; O'Donnell, G.E.; Robinson, A.J. Heat pipe-based radiator for low-grade geothermal energy conversion in domestic space heating. *Simul. Model. Pract. Theory* **2011**, *19*, 1154–1163. [CrossRef]
35. *GOST 32144-2013*; Electrical Energy. Electromagnetic Compatibility of Technical Equipment. Power Quality Limits in Public Power Supply Systems. Interstate Council for Standardization, Metrology and Certification: Minsk, Belarus, 2013.
36. Omron Corporation. *Technical Guide for Solid State Relays (CSM_SSR_TG_E_4_1)*; Omron Corporation: Kyoto, Japan, 2014.
37. Gefran S.p.A. *Solid State Relays, Contactors, and Power Controllers: Selection Guide*; Gefran S.p.A.: Provaglio d'Iseo, Italy, 2011.
38. On Approval of the Strategy for Achieving Carbon Neutrality of the Republic of Kazakhstan Until 2060. Decree of the President of the Republic of Kazakhstan No. 121, 2 February 2023. Available online: https://unfccc.int/sites/default/files/resource/Carbon_Neutrlaity_Strategy_Kazakhstan_Eng_Oct2024.pdf (accessed on 9 August 2026).
39. Kazakhstan Electricity Grid Operating Company (KEGOC). *Annual Report 2024*; KEGOC JSC: Astana, Kazakhstan, 2025.
40. International Energy Agency. *Clean Household Energy Consumption in Kazakhstan: A Roadmap*; International Energy Agency: Paris, France, 2020; 152p.
41. Lund, H.; Werner, S.; Wiltshire, R.; Svendsen, S.; Thorsen, J.E.; Hvelplund, F.; Mathiesen, B.V. 4th Generation District Heating (4GDH): Integrating smart thermal grids into future sustainable energy systems. *Energy* **2014**, *68*, 1–11.
42. Mukhtarov, R.; Ibragimova, O.P.; Omarova, A.; Tursumbayeva, M.; Tursun, K.; Muratuly, A.; Karaca, F.; Baimatova, N. An episode-based assessment for the adverse effects of air mass trajectories on PM2.5 levels in Astana and Almaty, Kazakhstan. *Urban Clim.* **2023**, *49*, 101541. [CrossRef]
43. Zlatev, V.; Cofala, J.; Peszko, G.; Wang, Q. *Clean Air and Cool Planet: Cost-Effective Air Quality Management in Kazakhstan and Its Impact on Greenhouse Gas Emissions*; Report No. AUS0002588; The World Bank: Washington, DC, USA, 2021.
44. Vafin, D.B. *Heat Supply and Heating Networks*; Nizhnekamsk Institute of Chemical Technology: Nizhnekamsk, Russia, 2014; 228p.
45. Sokolov, E.Y. *Heating and Heating Networks*, 7th ed.; MPEI Publishing House: Moscow, Russia, 2001; 472p.
46. Skanavi, A.N.; Makhov, L.M. *Heating*; DIA Publishing House: Moscow, Russia, 2008; 576p.
47. *SP RK 4.02-106-2013*; Autonomous Heat Supply Sources. Committee for Construction and Housing and Communal Services: Astana, Kazakhstan, 2019.
48. Kalinin, A.A. Parametric Optimization of the Electrotechnological Complex for Autonomous Heat Supply. Ph.D. Thesis, Karaganda State Technical University, Karaganda, Kazakhstan, 2018.
49. *SP RK 2.04-01-2017*; Construction Climatology. Committee for Construction and Housing and Communal Services: Astana, Kazakhstan, 2017.

50. International Energy Agency. *Kazakhstan—Countries & Regions: Electricity*; International Energy Agency: Paris, France, 2022.
51. Bureau of National Statistics of the Agency for Strategic Planning and Reforms of the Republic of Kazakhstan. *Fuel and Energy Balance of the Republic of Kazakhstan (2024)*; Bureau of National Statistics: Astana, Kazakhstan, 2025.
52. On Approval of the Concept for the Development of the Electric Power Industry of the Republic of Kazakhstan for 2023–2029. Resolution of the Government of the Republic of Kazakhstan No. 263, 28 March 2023. Available online: https://cis-legislation.com/document.fwx?rgn=149571 (accessed on 9 August 2026).
53. European Network of Transmission System Operators for Electricity (ENTSO-E). *Study on Power and Heat Sectors: Interactions and Synergies*; ENTSO-E: Brussels, Belgium, 2023.
54. International Renewable Energy Agency. *Power to Heat and Cooling: Status*; Innovation Landscape for Smart Electrification; IRENA: Abu Dhabi, United Arab Emirates, 2023.
55. Ma, Z.; Knotzer, A.; Billanes, J.D.; Jørgensen, B.N. A literature review of energy flexibility in district heating with a survey of the stakeholders' participation. *Renew. Sustain. Energy Rev.* **2020**, *123*, 109750. [CrossRef]
56. Luo, Z.; Peng, J.; Cao, J.; Yin, R.; Zou, B.; Tan, Y.; Yan, J. Demand flexibility of residential buildings: Definitions, flexible loads, and quantification methods. *Engineering* **2022**, *16*, 123–140. [CrossRef]
57. Goetzler, W.; Young, J.; Butrico, M.; Murphy, R. *Guidance Document on Space Heating Electrification for Large Commercial Buildings with Boilers*; U.S. Department of Energy: Washington, DC, USA, 2024.
58. Hewitt, N.J. Electrification of heating—Requirements for successful wide-scale deployment. *WIREs Energy Environ.* **2024**, *13*, e542. [CrossRef] [PubMed]
59. U.S. Department of Energy; National Renewable Energy Laboratory. *Saving Energy with Electric Resistance Heating*; DOE/GO-10097-381; U.S. Department of Energy: Washington, DC, USA, 1997.
60. Finck, C.; Li, R.; Kramer, R.; Zeiler, W. Quantifying demand flexibility of power-to-heat and thermal energy storage in the control of building heating systems. *Appl. Energy* **2018**, *209*, 409–425. [CrossRef]
61. Toropov, A.L.; Sargsyan, S.V. Energy efficiency of electric boilers of autonomous individual heat supply systems. *Vestn. MGSU* **2025**, *20*, 1104–1112.
62. Konovalov, N.P.; Shelekhov, I.Y. Design of an electric heating device for small rooms. *Bull. Irkutsk State Tech. Univ.* **2012**, *4*, 85–90.
63. Zhao, Z.; Hu, R.; Zhang, Y.; Dong, H.; Du, Q. Current research status and prospects of electrode boilers under the background of the "Dual Carbon" goals. *Energies* **2025**, *18*, 769. [CrossRef]
64. Shi, L.; Han, Z.; Feng, Y.; Zhang, C.; Zhang, Q.; Zhu, H.; Zhu, S. Joule heating of ionic conductors using zero-phase frequency alternating current to suppress electrochemical reactions. *Engineering* **2023**, *25*, 138–143. [CrossRef]
65. Korepanov, A.; Lekomtsev, P.; Niyazov, A. Energy characteristics of induction water heater. *IOP Conf. Ser. Earth Environ. Sci.* **2020**, *433*, 012035. [CrossRef]
66. Brown, K.J.; Farrelly, R.; O'Shaughnessy, S.M.; Robinson, A.J. Energy efficiency of electrical infrared heating elements. *Appl. Energy* **2016**, *162*, 581–588. [CrossRef]
67. Khan, A.; Irfan, M.; Niazi, U.M.; Shah, I.; Legutko, S.; Rahman, S.; Alwadie, A.S.; Jalalah, M.; Glowacz, A.; Khan, M.K.A. Centrifugal Compressor Stall Control by the Application of Engineered Surface Roughness on Diffuser Shroud Using Numerical Simulations. *Materials* **2021**, *14*, 2033. [CrossRef] [PubMed]
68. Bird, R.B.; Stewart, W.E.; Lightfoot, E.N. *Transport Phenomena*, 2nd ed.; John Wiley & Sons: New York, NY, USA, 2002.
69. Bergman, T.L.; Lavine, A.S.; Incropera, F.P.; DeWitt, D.P. *Fundamentals of Heat and Mass Transfer*, 8th ed.; John Wiley & Sons: Hoboken, NJ, USA, 2017.
70. Cotter, T.P. *Theory of Heat Pipes*; Los Alamos Scientific Laboratory Report LA-3246-MS; Los Alamos Scientific Laboratory: Los Alamos, NM, USA, 1965.
71. Nield, D.A.; Bejan, A. *Convection in Porous Media*, 5th ed.; Springer: Cham, Switzerland, 2017. [CrossRef]
72. Wagner, W.; Pruß, A. The IAPWS formulation 1995 for the thermodynamic properties of ordinary water substance for general and scientific use. *J. Phys. Chem. Ref. Data* **2002**, *31*, 387–535. [CrossRef]
73. Wagner, W.; Cooper, J.R.; Dittmann, A.; Kijima, J.; Kretzschmar, H.-J.G.; Mareš, R.; Oguchi, K.; Sato, H.; Stock, J.; Takaishi, Y.; et al. The IAPWS industrial formulation 1997 for the thermodynamic properties of water and steam. *J. Eng. Gas Turbines Power* **2000**, *122*, 150–184. [CrossRef]
74. Shabgard, H.; Allen, M.J.; Sharifi, N.; Benn, S.P.; Faghri, A.; Bergman, T.L. Heat pipe heat exchangers and heat sinks: Opportunities, challenges, applications, analysis, and state of the art. *Int. J. Heat Mass Transf.* **2015**, *89*, 138–158. [CrossRef]
75. Ranjan, R.; Murthy, J.Y.; Garimella, S.V.; Vadakkan, U. A numerical model for transport in flat heat pipes considering wick microstructure effects. *Int. J. Heat Mass Transf.* **2011**, *54*, 153–168. [CrossRef]
76. Kaya, T.; Goldak, J. A mathematical model for analyzing the thermal characteristics of a flat micro heat pipe with a grooved wick. *Int. J. Heat Mass Transf.* **2008**, *51*, 4637–4650. [CrossRef]
77. Sangpab, N.; Sakulchangsatjatai, P.; Kammuang-lue, N.; Terdtoon, P. Mathematical model of bent-flattened sintered-grooved heat pipe with concept of receding-and-excessing fluid. *Case Stud. Therm. Eng.* **2021**, *27*, 101307. [CrossRef]

78. Nusselt, W. Die Oberflächenkondensation des Wasserdampfes. *Z. Ver. Dtsch. Ing.* **1916**, *60*, 541–546, 569–575.
79. Harvey, A.H. *Thermodynamic Properties of Water: Tabulation from the IAPWS Formulation 1995*; NISTIR 5078; National Institute of Standards and Technology: Gaithersburg, MD, USA, 1998.
80. Kalytka, V.; Mekhtiyev, A.; Neshina, Y.; Yurchenko, A.; Alkina, A.; Bulatbayev, F.; Issayev, V.; Makhanov, K.; Lukin, D.; Kayumov, D.; et al. Nonlinear quasi-classical model of isothermal relaxation polarization currents in functional elements of microelectronics, optoelectronics and fiber optics based on crystals with ionic-molecular chemical bonds with complex crystalline structure. *Crystals* **2025**, *15*, 863. [CrossRef]
81. Kalytka, V.; Bulatbayev, F.; Neshina, Y.; Bilichenko, Y.; Bilichenko, A.; Bashirov, A.; Sidorina, Y.; Naboko, Y.; Malikov, N.; Senina, Y. Theoretical studies of nonlinear relaxation electrophysical phenomena in dielectrics with ionic-molecular chemical bonds in a wide range of fields and temperatures. *Appl. Sci.* **2022**, *12*, 6555. [CrossRef]
82. Kalytka, V.; Baimukhanov, Z.; Neshina, Y.; Mekhtiyev, A.; Dunayev, P.; Galtseva, O.; Senina, Y. Influence of quantum effects on dielectric relaxation in functional electrical and electric energy elements based on proton semiconductors and dielectrics. *Appl. Sci.* **2023**, *13*, 8755. [CrossRef]
83. Kalytka, V.; Mekhtiyev, A.; Neshina, Y.; Alkina, A.; Aimagambetova, R.; Mukhambetov, G.; Bashirov, A.; Afanasyev, D.; Bilichenko, A.; Zhumagulova, D.; et al. Physical and mathematical models of quantum dielectric relaxation in electrical and optoelectric elements based on hydrogen-bonded crystals. *Crystals* **2023**, *13*, 1353. [CrossRef]
84. Kalytka, V.; Mekhtiyev, A.; Neshina, Y.; Alkina, A.; Senina, Y.; Bilichenko, A.; Sidorina, Y.; Beissekov, A.; Tatkeyeva, G.; Sarsikeyev, Y. Quasi-classical models of nonlinear relaxation polarization and conductivity in electric, optoelectric, and fiber optic elements based on materials with ionic-molecular chemical bonds. *Appl. Sci.* **2024**, *14*, 11830. [CrossRef]

Disclaimer/Publisher's Note: The statements, opinions and data contained in all publications are solely those of the individual author(s) and contributor(s) and not of MDPI and/or the editor(s). MDPI and/or the editor(s) disclaim responsibility for any injury to people or property resulting from any ideas, methods, instructions or products referred to in the content.